



Adaptive Fuzzy PI Output Feedback Control for a Class of Switched Nonlinear Systems with Unmodeled Dynamics and Dead-Zone Output

Hongyao Li¹ · Haibin Sun¹ · Linlin Hou²

Received: 11 January 2021 / Revised: 16 July 2021 / Accepted: 5 August 2021 / Published online: 28 August 2021
© Taiwan Fuzzy Systems Association 2021

Abstract In this paper, the problem of adaptive fuzzy proportional-integral output feedback tracking control is investigated for a class of uncertain switched nonlinear systems with dead-zone output, unknown control coefficients, and unmodeled dynamics. The unknown parameter of the dead-zone output is processed using adaptive estimation technique. A set of switched filters are developed to estimate unmeasurable states. Then, by combining fuzzy logic systems and backstepping technique, an adaptive output feedback PI tracking controller is developed, which has intuitive structure and a strong physical meaning. Finally, the boundedness of the tracking error and all signals in the closed-loop system is demonstrated via a multiple Lyapunov function. The effectiveness of the proposed scheme is confirmed through two examples.

Keywords Backstepping · Dead-zone output · FLSs · PI control · Switched nonlinear system · Unmodeled dynamics

1 Introduction

In recent decades, switched systems are investigated because they can be used to model many practical systems [1–15], such as, robot control systems [16–18], flight systems [19, 20], and network systems [21–24]. It is well-

known that switched systems consist of multiple subsystems and a switching rule. Because the stability of a subsystem does not determine the stability of the switched system, a variety of stability analysis tools are developed to analyze the stability of switched systems, such as common Lyapunov function, multiple Lyapunov function, and single Lyapunov function. Subsequently, a large number of research results are reported. For example, in [25], the tracking control problem is researched for switched nonlinear systems by adopting the common Lyapunov function. By designing a set of switched state observers to estimate the unknown states, an adaptive fuzzy output-feedback controller is constructed in [26] for nonstrict feedback switched nonlinear systems. In [27], the tracking control problem is investigated for switched nonlinear systems via dynamic surface control method. Recently, the adaptive neural tracking control problem for a class of nonlower triangular uncertain switched stochastic nonlinear pure feedback systems is studied in [28]. In [29], an adaptive nonlinear disturbance observer strategy is proposed for switched uncertain pure feedback nonlinear systems with mismatched external disturbances and arbitrary switching. However, the above literature does not take into account unmodeled dynamics.

Unmodeled dynamics is common in engineering environment owing to the wide existence of modeling errors and external disturbances. If the unmodeled dynamics are neglected, the closed-loop system performance will be destroyed [30]. Therefore, numerous studies are researched for switched nonlinear systems with unmodeled dynamics [31–34]. In [31], a novel robust adaptive stabilization control scheme is proposed by employing a small-gain approach. Two types of unmodeled dynamics, namely stable and unstable, are considered by constructing the multiple Lyapunov function in [32]. Aiming at time-delay

✉ Haibin Sun
seusunhaibin@gmail.com

¹ School of Engineering, Qufu Normal University, Rizhao 276826, Shandong, People's Republic of China

² School of Information Science and Engineering, Qufu Normal University, Rizhao 276826, Shandong, People's Republic of China

systems, an adaptive fuzzy prescribed performance control scheme is introduced in [33]. An adaptive neural tracking controller is developed for interconnected switched systems in [34]. On the other hand, unknown control coefficients are one of the serious uncertainties in nonlinear systems. In [25], a tracking control scheme is developed for switched nonlinear systems with unknown control coefficients. The problem of output feedback bounded control is studied for a class of switched nonlinear uncertain systems in [35]. However, the aforementioned studies are restricted; they do not consider the influence of system constraints. System constraints, such as actuator saturation, state constraints, and dead-zone output. These constraints widely exist in practical engineering systems. Owing to the limitations in the physical properties of the components, the dead-zone as one of the nonsmooth nonlinearities often found in physical systems. The existing dead-zone may seriously affect the system performance. This inspires studies on the control problem of nonlinear systems with a dead-zone output. For instance, an adaptive fuzzy output feedback dynamic surface control scheme is developed for nonlinear systems in [36]. In [37], an adaptive tracking controller is designed for nonstrict feedback nonlinear systems with input saturation and unknown output dead-zone by introducing the Nussbaum-type function. In [38], the adaptive neural tracking control problem is studied for switched nonlinear systems with unknown backlash-like hysteresis and output dead-zone. Although good control performance is obtained in the aforementioned schemes, the effect of unmodeled dynamics is not considered and the controller is relatively complex.

PI control, as a control scheme with a simple and intuitive structure and strong physical significance, is popular in practical engineering applications. In the early days, a novel compensator identification scheme is proposed in [39] to address the problem of factory identification. Subsequently, for linear systems, a proportional-integral-differential (PID) gain self-tuning technique is proposed in [40]. In [41], a PI/PID control scheme is first developed for nonlinear systems. However, derivative control has an evident drawback, i.e., it is easy to introduce high-frequency noise. Therefore, many studies focus on PI control, which not only avoids the aforementioned defects, but also simplifies the controller structure and significantly reduces the calculation cost. In [42, 43], the intelligent PI (iPI) controllers are investigated for a class of flexible-link manipulator. For the purpose of addressing the tracking control problem for multiple-input-multiple-output (MIMO) nonlinear system with dead-zone input, a PI

control scheme is designed in [44]. Aiming at non-affine systems with actuator and sensor faults, a PI controller is proposed to handle the tracking control problem in [45]. In [46], a PI structure controller is constructed by defining the generalized error at each step of the backstepping method. In recent years, a decentralized adaptive neural network PI tracking control scheme is proposed in [47] for interconnected nonlinear systems with input quantization and dynamic uncertainty. Note that the aforementioned studies on the problem of PI control does not involve switched systems, which inspires us to investigate the PI control problem of the switched nonlinear systems. To sum up, it is necessary to study the problem of PI control for switched nonlinear systems with unmodeled dynamics, unknown control coefficients, and dead-zone output. To solve this problem, three key points need to be addressed: (i) how to design a controller with a PI structure for switched nonlinear systems with unmodeled dynamics, unknown control coefficients, and dead-zone output? (ii) how to deal with unknown information of the dead-zone output and unknown control coefficient? (iii) how to compensate the nonlinear term caused by the construction of the virtual control law and controller at each step?

This paper addresses the problem of adaptive fuzzy PI output feedback control for a class of uncertain switched nonlinear systems with unmodeled dynamics, unknown control coefficients, and dead-zone output. An adaptive fuzzy PI output feedback controller is proposed by applying the backstepping method and FLSs. The boundedness of the tracking error and all signals in the closed-loop system are demonstrated via Lyapunov stability theory. The main contributions can be summarized as follows.

- An adaptive fuzzy PI controller for uncertain switched nonlinear systems with unmodeled dynamics, unknown control coefficients, and dead-zone output is proposed for the first time; this controller features an intuitive structure and a strong physical meaning.
- The difficulty of unknown parameter of the dead-zone is overcome by adaptive estimation.
- The properties of the hyperbolic tangent function and FLSs are flexibly employed to deal with the nonlinear terms generated by constructing the virtual control law and control law.

The remainder of this paper is organised as follows. Section 2 presents the problem formulation. In Sect. 3, the switched filters, adaptive fuzzy PI controller and stability analysis of the closed-loop systems are presented. Section 4 provides two examples that verify the effectiveness of the scheme. Section 5 concludes the paper.

2 Problem Formulation and Preliminaries

2.1 Problem Formulation

Consider the following switched nonlinear systems with unmodeled dynamics

$$\begin{aligned} \dot{\varsigma} &= q_{\sigma(t)}(\varsigma, y, d(t)), \\ \dot{x}_1 &= h_1 x_2 + f_{1,\sigma(t)}(x_1) + \Delta_{1,\sigma(t)}(\varsigma, y, d(t)), \\ \dot{x}_2 &= h_2 x_3 + f_{2,\sigma(t)}(x_1, x_2) + \Delta_{2,\sigma(t)}(\varsigma, y, d(t)), \\ &\vdots \\ \dot{x}_n &= h_n u + f_{n,\sigma(t)}(x_1, x_2, \dots, x_n) + \Delta_{n,\sigma(t)}(\varsigma, y, d(t)), \\ y &= D(x_1), \end{aligned} \quad (1)$$

where $x = [x_1, x_2, \dots, x_n]^T \in R^n$ are the system states, u is the control input and $y = D(x_1)$ denotes the output with dead-zone, ς represents an unmodeled dynamic, and h_1, h_2, \dots, h_n are positive constants that represents the unknown control coefficients. Besides, $\sigma(t) : [0, +\infty) \rightarrow \mathcal{P} = \{1, 2, \dots, p\}$ denotes the switching signal. For any $i = 1, 2, \dots, n$ and $k \in \mathcal{P}$, $f_{i,k}$ and $q_k(\varsigma, y, d(t))$ are uncertain functions, and $\Delta_{i,k}(\varsigma, y, d(t))$ represent unknown functions called non-parametric uncertainties, $d(t)$ means an unknown disturbance.

In system (1), the dead-zone output y is represented as

$$y = D(x_1) = \begin{cases} l(x_1 - v), & x_1 > v \\ 0, & -v \leq x_1 \leq v \\ l(x_1 + v), & x_1 < -v, \end{cases} \quad (2)$$

where $l > 0$ denotes the slope of the dead-zone and $v > 0$ represents the width parameter.

Similar to the treatment of the dead-zone output in [38], (2) can be approximated as

$$x_1 = \frac{y}{l} + \frac{2v}{\pi} \arctan(ay), \quad (3)$$

where a is a positive constant. Then

$$\frac{dx_1}{dy} = \frac{1}{l} + \frac{2v}{\pi} \frac{a}{1 + (ay)^2}. \quad (4)$$

We can further obtain $\dot{y} = \frac{dy}{dx_1} \dot{x}_1 = \check{\beta} \dot{x}_1$, $\frac{l\pi}{\pi+2vay} \leq \check{\beta} = \frac{dy}{dx_1} < l$.

Remark 1 Note that (2) is a non-smooth model. The non-smooth dead-zone nonlinearity in (2) can be approximated by (3). As the parameter a increases, the model represented by (3) is closer to the system output (2), as shown in Fig. 1.

Remark 2 Define $h = h_1 h_2 \dots h_n$. It is clear that $\check{\beta} h$ is bounded. Consequently, there exist two positive constants $\bar{\beta}_1$ and $\bar{\beta}_2$ such that $\bar{\beta}_1 < \check{\beta} h < \bar{\beta}_2$.

Adaptive PI fuzzy output feedback tracking control

problem: In this paper, an adaptive PI fuzzy output feedback tracking controller will be designed by the backstepping method for system (1), such that the system output y tracks the reference signal y_d and all signals of the closed-loop system are bounded.

Assumption 1 $y_d, \dot{y}_d, \dots, y_d^{(n)}$ are smooth and bounded.

Assumption 2 [33] The subsystem $\dot{\varsigma} = q_{\sigma(t)}(\varsigma, y, d(t))$ is input-to-state stable (ISS) with input y . An ISS-Lyapunov function V_ς satisfies

$$\beta_1(|\varsigma|) \leq V_\varsigma(\varsigma) \leq \beta_2(|\varsigma|), \quad \frac{\partial V_\varsigma}{\partial \varsigma} \dot{\varsigma} \leq -a_0 V_\varsigma + n_0 \gamma(|y|), \quad (5)$$

where β_1, β_2, γ belong to class- \mathcal{K}_∞ , a_0 and $n_0 > 0$ are unknown positive constants, where $\gamma(s) = O(s^2)$, and “ O ” denotes that there exist $m > 0$ and $n > 0$, for any $|s| < n$, such that $|\gamma(s)| \leq m|s|^2$.

Assumption 3 [48] The nonlinear function $\Delta_{i,k}(\varsigma, y, d(t))$ satisfies

$$|\Delta_{i,k}(\varsigma, y, d(t))| \leq w_{ik} \varphi_{i1}(|\varsigma|) + w_{ik} \varphi_{i2}(y), \quad (6)$$

where w_{ik} are unknown constants, $\varphi_{i1}(|\varsigma|)$, and $\varphi_{i2}(y)$ are smooth functions that satisfy $\varphi_{i1}(0) = 0$, $\varphi_{i2}(0) = 0$. Similar to [48], we can obtain $\varphi_{i2}(y) = y \bar{\varphi}_{i2}(y)$ ($\bar{\varphi}_{i2}(y)$ is a smooth function) and the following property [33] holds

$$\limsup_{\iota \rightarrow 0^+} \frac{\varphi_{i1}^2(|\varsigma|)}{V_\varsigma} < +\infty. \quad (7)$$

Lemma 1 [49] $f(X)$ is a continuous function defined on a compact set \mathcal{K} , and there exists FLSs $y = \Phi^T S(X)$ such that $\sup_{X \in \mathcal{K}} |f(X) - \Phi^T S(X)| \leq \varepsilon$,

where Φ represents the weight of the FLSs, $S(X)$ is a basis function vector, and $\varepsilon > 0$ is a prescribed accuracy.

Lemma 2 [50] For any $1 \leq i \leq n$, define the set $\mathcal{E}_{\chi_i} = \{\chi_i \mid \|\chi_i\| < \iota \varpi_i\}$, where $\iota = 0.8814$ and $\varpi_i > 0$. Then, if $\chi_i \notin \mathcal{E}_{\chi_i}$, the inequality $[1 - 2 \tanh^2(\frac{\chi_i}{\varpi_i})] \leq 0$ holds.

Remark 3 Note that many studies have been investigated on PI control for nonswitched nonlinear systems [47, 51]. However, in practical situations, switching behavior and unmodeled dynamics widely exist in many systems. Hence, it is important to study PI control for switched nonlinear systems with unmodeled dynamics.

Remark 4 From Lemma 1, we can conclude that the following conclusion: $f(\chi) = \Phi^T S(X) + \vartheta$, where ϑ is a bounded function that satisfies $|\vartheta| \leq \varepsilon$ and $S(X)$ satisfies: $0 < S(X)^T S(X) \leq 1$.

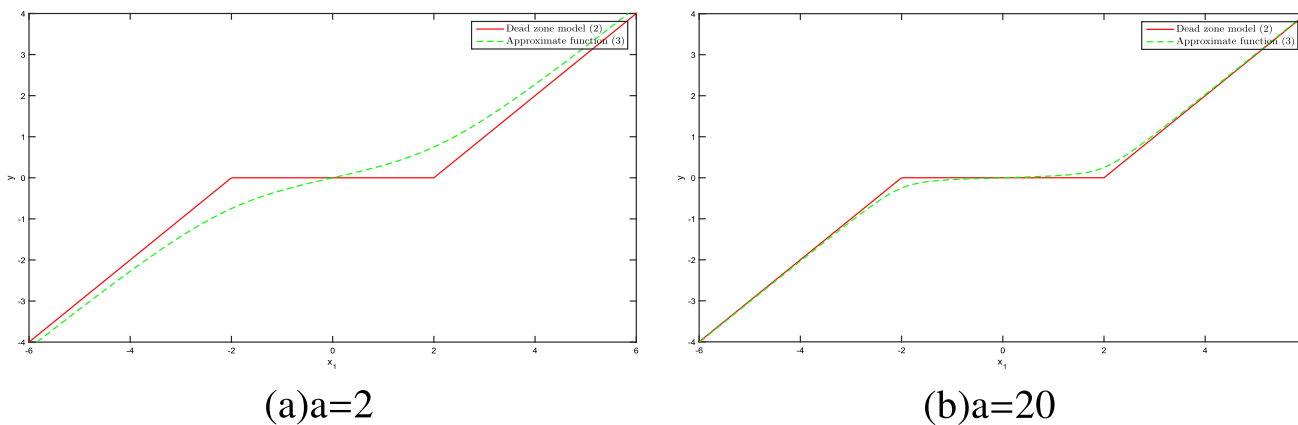


Fig. 1 Curves of y when a = 2 and a = 20

3 Main Results

3.1 Design of Filters

To manage unknown control coefficients, the following variables are defined

$$\zeta_i = \frac{x_i}{h_i \dots h_n}, f_{i,k}^* = \frac{f_{i,k}}{h_i \dots h_n}, \Delta_{i,k}^* = \frac{\Delta_{i,k}}{h_i \dots h_n}.$$

Then we have

$$\begin{aligned} \dot{\zeta}_1 &= \zeta_2 + f_{1,k}^* + \Delta_{1,k}^*, \\ \dot{\zeta}_2 &= \zeta_3 + f_{2,k}^* + \Delta_{2,k}^*, \\ &\dots \\ \dot{\zeta}_n &= u + f_{n,k}^* + \Delta_{n,k}^*. \end{aligned} \tag{9}$$

Construct a set of filters as

$$\begin{aligned} \dot{\hat{\zeta}}_1 &= \hat{\zeta}_2 - \mu_{1,k} \hat{\zeta}_1, \\ \dot{\hat{\zeta}}_2 &= \hat{\zeta}_3 - \mu_{2,k} \hat{\zeta}_1, \\ &\dots \\ \dot{\hat{\zeta}}_n &= u - \mu_{n,k} \hat{\zeta}_1, \end{aligned} \tag{10}$$

where $\mu_{1,k}, \mu_{2,k}, \dots, \mu_{n,k}$ are positive constants. Define the error variables as $\tilde{\zeta}_i = \zeta_i - \hat{\zeta}_i$. Combining (9) with (10) leads to

$$\dot{\tilde{\zeta}} = A_k \tilde{\zeta} + F_k^* + \Delta_k^* + \frac{1}{h} U_k x_1, \tag{11}$$

where
$$A_k = \begin{pmatrix} -\mu_{1,k} & & & \\ \vdots & I_{n-1} & & \\ \mu_{n,k} & \dots & 0 & \end{pmatrix}, \quad F_k^* = \begin{pmatrix} f_{1,k}^* \\ \vdots \\ f_{n,k}^* \end{pmatrix},$$

$$\Delta_k^* = \begin{pmatrix} \Delta_{1,k}^* \\ \vdots \\ \Delta_{n,k}^* \end{pmatrix}, \quad U_k = \begin{pmatrix} \mu_{1,k} \\ \vdots \\ \mu_{n,k} \end{pmatrix}.$$

Define $w^* = \max\{1, \frac{w_{i,k}}{h_i \dots h_n}, \frac{1}{h}\}$ and $e = \frac{1}{w^*} \tilde{\zeta}$. Then one has

$$\begin{aligned} \dot{e} &= q_{\sigma(t)}(e, y), \\ \dot{e} &= A_k e + \frac{1}{w^*} F_k^* + \frac{1}{w^*} \Delta_k^* + \frac{1}{w^*} \frac{1}{h} U_k x_1, \\ \dot{x}_1 &= h \hat{\zeta}_2 + h w^* e_2 + f_{1,k}^* + \Delta_{1,k}^*, \\ \dot{\hat{\zeta}}_1 &= \hat{\zeta}_2 - \mu_{1,k} \hat{\zeta}_1, \\ \dot{\hat{\zeta}}_2 &= \hat{\zeta}_3 - \mu_{2,k} \hat{\zeta}_1, \\ &\dots \\ \dot{\hat{\zeta}}_n &= u - \mu_{n,k} \hat{\zeta}_1. \end{aligned} \tag{12}$$

Choose the appropriate parameter $\mu_{i,k}$ such that A_k is a Hurwitz matrix. Hence there exists a positive definite symmetric matrix P_k such that

$$A_k^T P_k + P_k A_k = -2I. \tag{13}$$

Choosing $V_k^* = e^T P_k e$ and calculating the derivative of V_k^* yield

$$\dot{V}_k^* = -2e^T e + 2e^T P_k \frac{1}{w^*} F_k^* + 2e^T P_k \frac{1}{w^*} \Delta_k^* + 2e^T P_k \frac{1}{w^*} \frac{1}{h} U_k x_1. \tag{14}$$

According to Remark 4, we obtain $F_k^* = \Phi_{0,k}^T S_{0,k} + \vartheta_{0,k}$, $\Phi_{0,k} = [\Phi_{01,k}, \Phi_{02,k}, \dots, \Phi_{0n,k}]$, $S_{0,k}$ is a basis function vector, $\vartheta_{0,k} = [\vartheta_{01,k}, \vartheta_{02,k}, \dots, \vartheta_{0n,k}]$, where $\Phi_{0i,k}$ are the weights, and $\vartheta_{0i,k}$ are bounded functions that satisfy $\|\vartheta_{0,k}\| \leq \varepsilon_{0,k}$, where $\varepsilon_{0,k}$ is a positive constant. Then the following inequations is derived

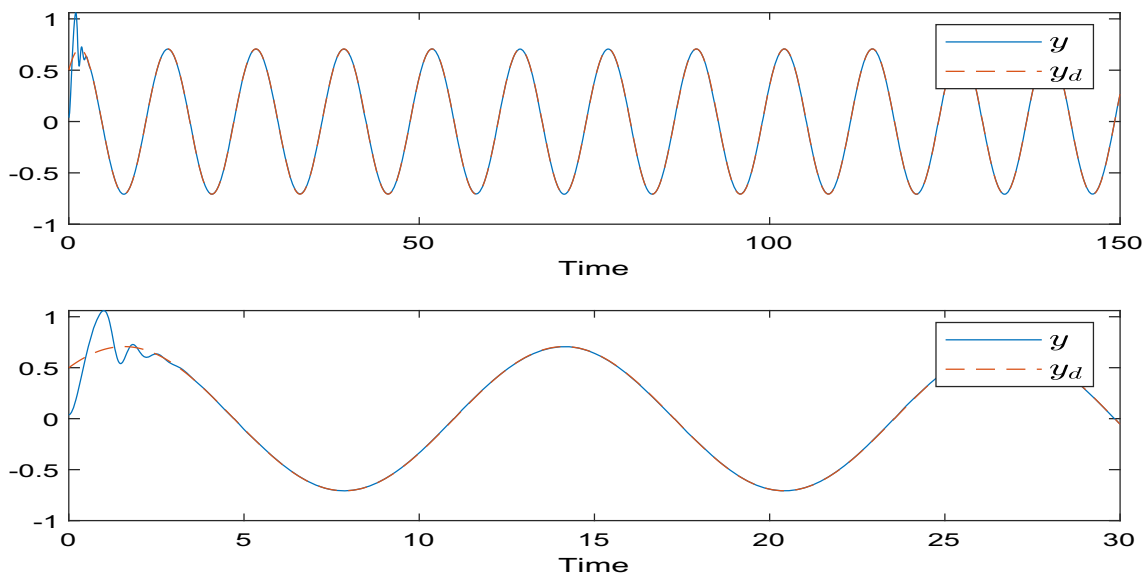


Fig. 2 Curves of y and y_d for Example 1

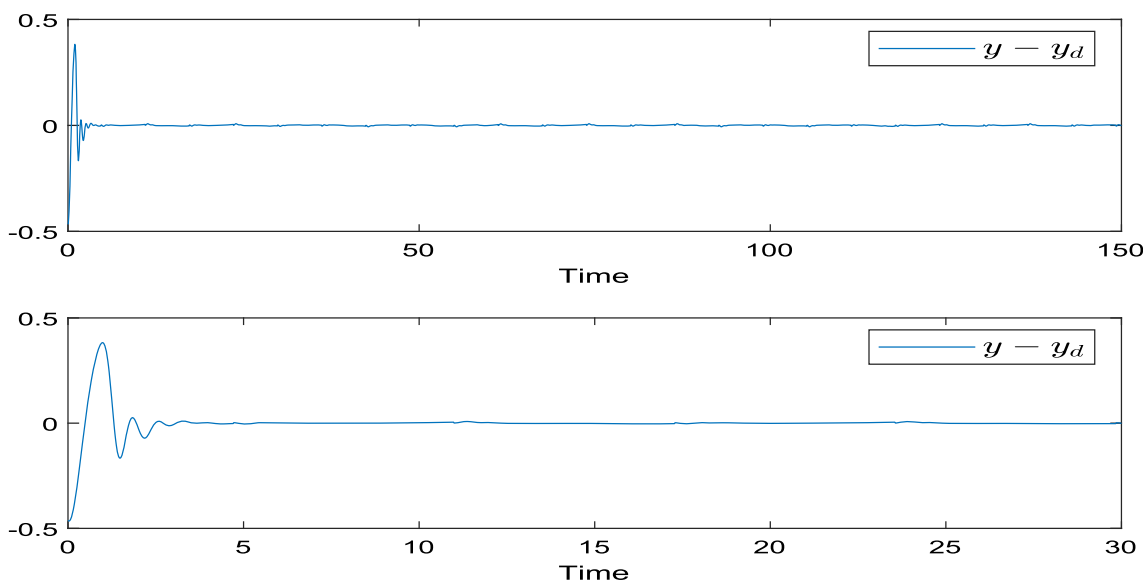


Fig. 3 Curve of tracking error $y - y_d$ for Example 1

$$\begin{aligned}
 2e^T P_k \frac{1}{w^*} F_k^* &= 2e^T P_k \frac{1}{w^*} (\Phi_{0,k}^T S_0 + \vartheta_{0,k}) \\
 &= 2e^T P_k \frac{1}{w^*} \Phi_{0,k}^T S_0 + 2e^T P_k \frac{1}{w^*} \vartheta_{0,k} \\
 &\leq \frac{1}{4} e^T e + 8 \|P_k\|^2 \frac{1}{w^{*2}} (\theta + \varepsilon_{0,k}^2),
 \end{aligned}
 \tag{15}$$

$$\begin{aligned}
 2e^T P_k \frac{1}{w^*} \Delta_k^* &\leq \frac{1}{4} e^T e + 8 \|P_k\|^2 \sum_{i=1}^n \varphi_{i,1}^2 (|\varsigma|) \\
 &\quad + 8 \|P_k\|^2 \sum_{i=1}^n y^2 \bar{\varphi}_{i,2}^2 (y),
 \end{aligned}
 \tag{16}$$

$$\begin{aligned}
 2e^T P_k \frac{1}{w^* h} U_k x_1 &= 2e^T P_k \frac{1}{w^* h} U_k \left(\frac{y}{l} + \frac{2v}{\pi} \arctan(ay) \right) \\
 &\leq \frac{1}{4} e^T e + 8 \|P_k\|^2 \|U_k\|^2 \frac{1}{l^2} y^2 + 8 \|P_k\|^2 \|U_k\|^2 v^2,
 \end{aligned}
 \tag{17}$$

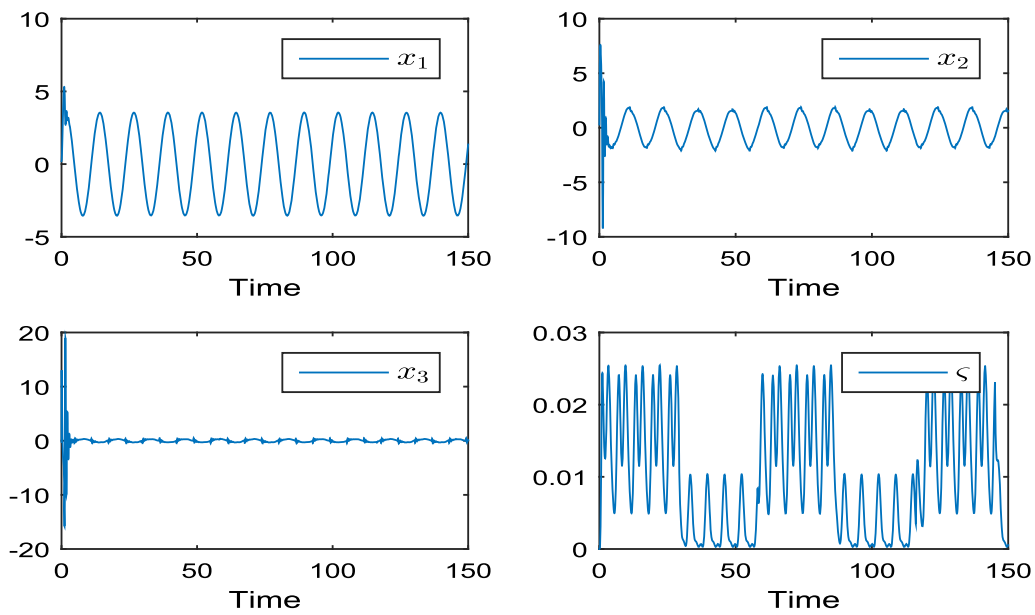


Fig. 4 Curves of x_1, x_2, x_3 and ζ for Example 1

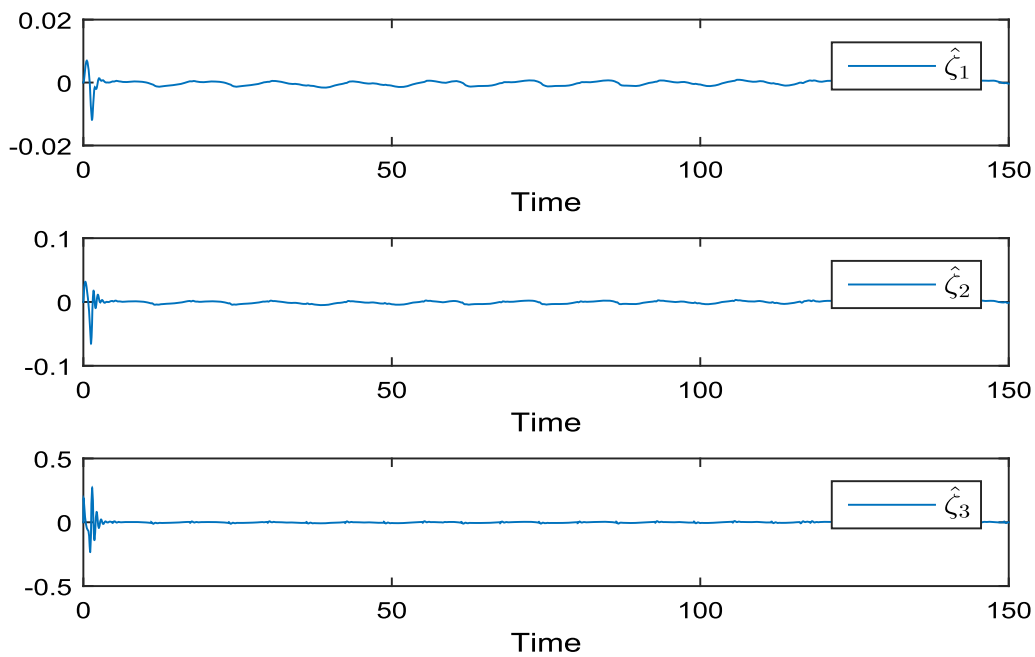


Fig. 5 Curves of $\hat{\zeta}_1, \hat{\zeta}_2$ and $\hat{\zeta}_3$ for Example 1

where $\theta = \max\{\|\Phi_{i,k}\|^2 : 0 \leq i \leq n, k \in \mathcal{P}\}$, and $\Phi_{i,k}$ mean the weights of FLSs.

Combining (14), (15), (16) with (17) leads to

$$\begin{aligned} \dot{V}_k^* \leq & -e^T e + b_k \gamma^2 \left(\sum_{i=1}^n \bar{\varphi}_{i,2}^2(y) + 1 \right) \\ & + 8\|P_k\|^2 \sum_{i=1}^n \varphi_{i,1}^2(|\zeta|) + d_{0,k}, \end{aligned} \tag{18}$$

where $b_k = 8\|P_k\|^2 \cdot \max\{1, \frac{1}{\rho^2} \|U_k\|^2\}$, $d_{0,k} = 8\|P_k\|^2 \frac{1}{w^{*2}} (\theta + \bar{e}_{0,k}^2) + 8\|P_k\|^2 \|U_k\|^2 v^2$.

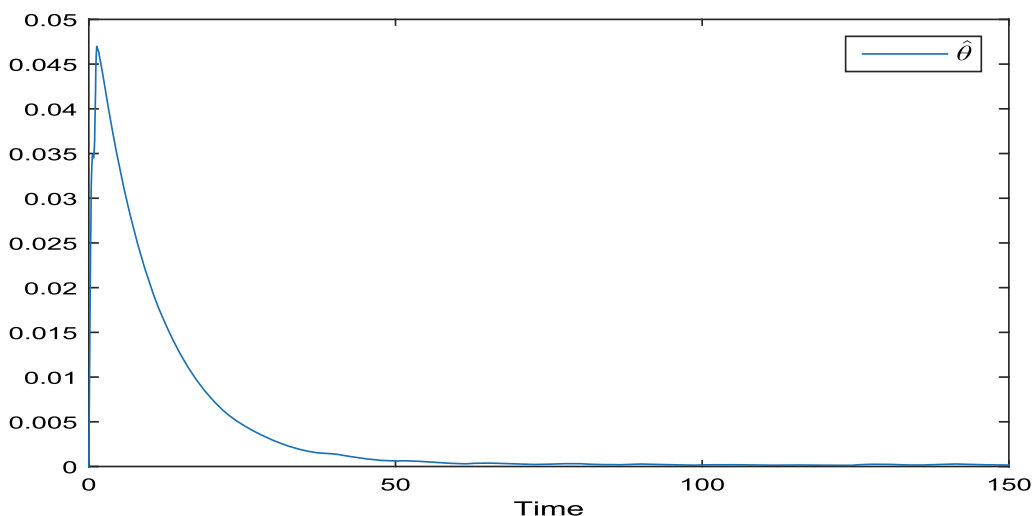


Fig. 6 Curve of $\hat{\theta}$ for Example 1

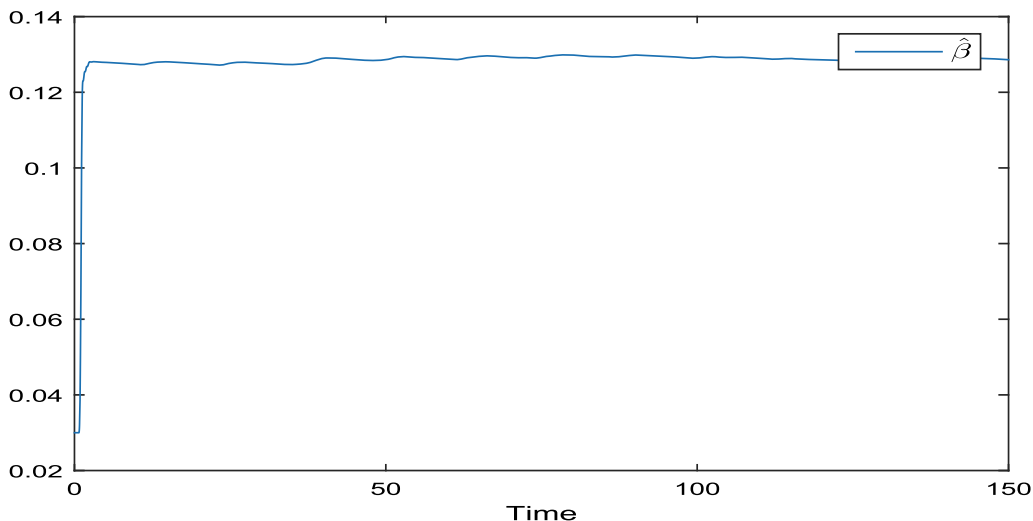


Fig. 7 Curve of $\hat{\beta}$ for Example 1

3.2 Controller Design

First, a set of coordinate transformations are defined:

$$\begin{aligned} r_1 &= y - y_d, \\ r_2 &= \hat{\zeta}_2 - \alpha_1, \\ &\vdots \\ r_n &= \hat{\zeta}_n - \alpha_{n-1}, \end{aligned}$$

where $\alpha_1, \dots, \alpha_{n-1}$ are the virtual control laws and the following generalized errors are further introduced:

$$\begin{aligned} \chi_1 &= r_1 + s_1 \int_0^t r_1 d\tau, \\ \chi_2 &= r_2 + s_2 \int_0^t r_2 d\tau, \\ &\vdots \\ \chi_n &= r_n + s_n \int_0^t r_n d\tau, \end{aligned}$$

where s_1, \dots, s_n are positive constants.

In this paper, the virtual control laws are constructed as

$$\alpha_1 = \hat{\beta} \bar{\alpha}_1, \tag{19}$$

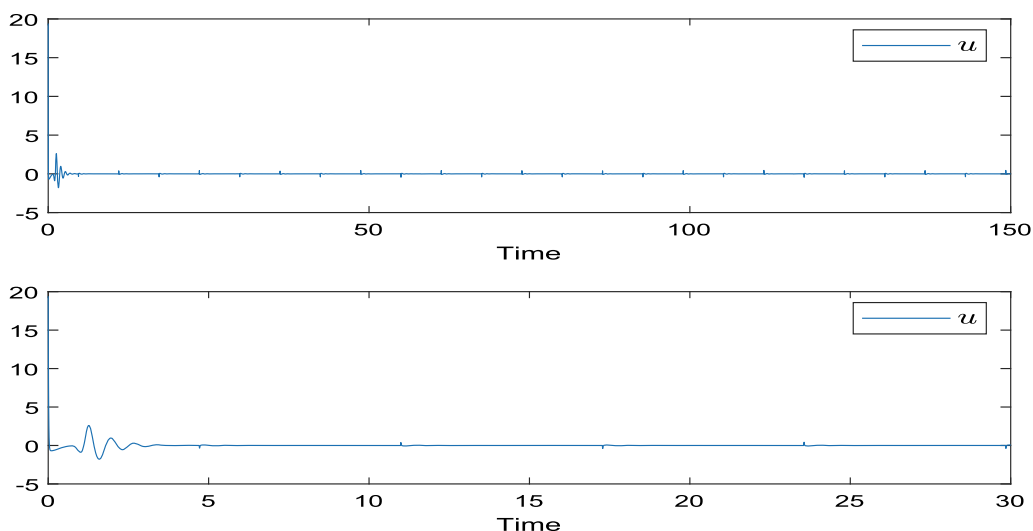


Fig. 8 Curve of control input u for Example 1

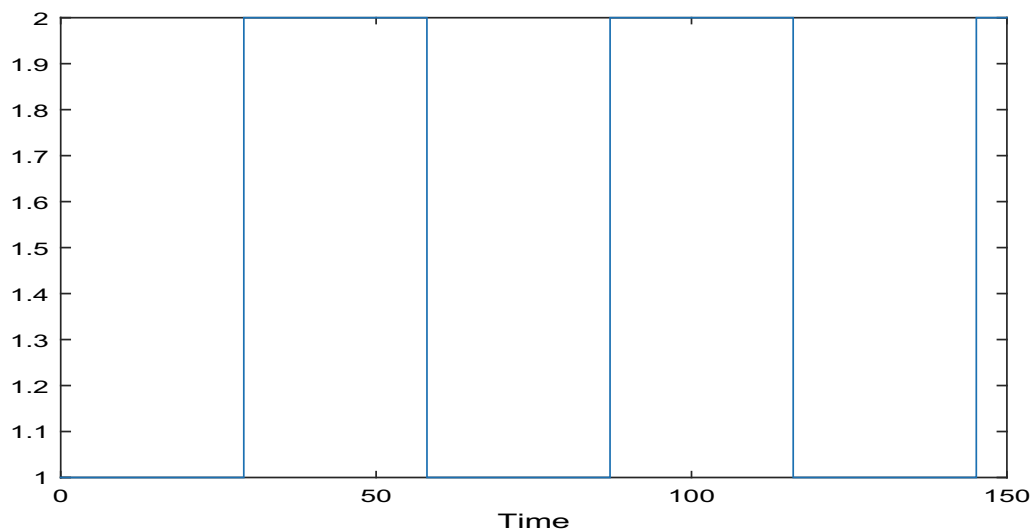


Fig. 9 Curve of the switching signal for Example 1

$$\bar{\alpha}_1 = -(g_{P_1} + \Delta g_{P_1}(\cdot))r_1 - (g_{I_1} + \Delta g_{I_1}(\cdot)) \int_0^t r_1 d\tau, \tag{20}$$

$$\alpha_i = -(g_{P_i} + \Delta g_{P_i}(\cdot))r_i - (g_{I_i} + \Delta g_{I_i}(\cdot)) \int_0^t r_i d\tau, \tag{21}$$

for any $i = 1, \dots, n - 1$, $g_{P_i} = c_i$, $g_{I_i} = s_i g_{P_i}$, $\Delta g_{P_i}(\cdot) = \frac{\hat{\theta}}{2a_i^2}$, $\Delta g_{I_i}(\cdot) = s_i \Delta g_{P_i}(\cdot)$, $\hat{\theta}$ is the estimation of θ , $\hat{\beta}$ is the estimation of β , where $\beta = \frac{1}{\beta_1}$. a_i, c_i are the positive constants.

The adaptive PI controller is designed as

$$u = -(g_{P_n} + \Delta g_{P_n}(\cdot))r_n - (g_{I_n} + \Delta g_{I_n}(\cdot)) \int_0^t r_n d\tau, \tag{22}$$

where $g_{P_n} = c_n$, $g_{I_n} = s_n g_{P_n}$, $\Delta g_{P_n}(\cdot) = \frac{\hat{\theta}}{2a_n^2}$, $\Delta g_{I_n}(\cdot) = s_n \Delta g_{P_n}(\cdot)$, a_n, c_n are the positive constants.

The adaptive laws are designed as:

$$\dot{\hat{\theta}} = \sum_{i=1}^n \frac{j\chi_i^2}{2a_i^2} - \hbar \hat{\theta}, \tag{23}$$

$$\dot{\hat{\beta}} = Proj(\hat{\beta}(t), \Xi), \tag{24}$$

$$Proj(\hat{\beta}(t), \Xi) = \begin{cases} 0, & \text{if } \hat{\beta} = \hat{\beta}_{\max} \wedge \Xi > 0 \\ 0, & \text{if } \hat{\beta} = \hat{\beta}_{\min} \wedge \Xi < 0 \\ \Xi, & \text{otherwise} \end{cases}, \tag{25}$$

where $\Xi = (c_1 + \frac{\hat{\theta}}{2a_1^2})\chi_1^2 - \iota \hat{\beta}$, j, \hbar, ι are positive constants.

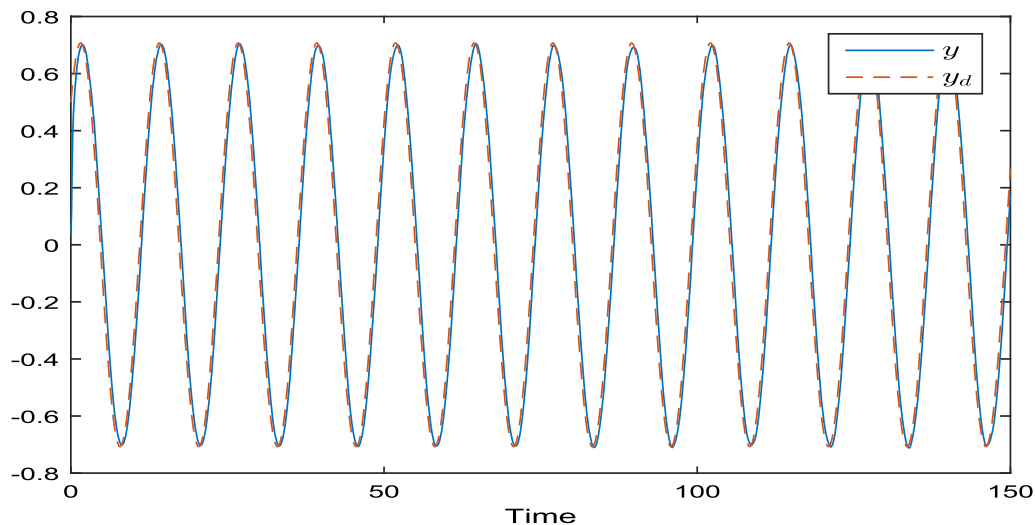


Fig. 10 Curves of y and y_d for scheme 2 in Example 1

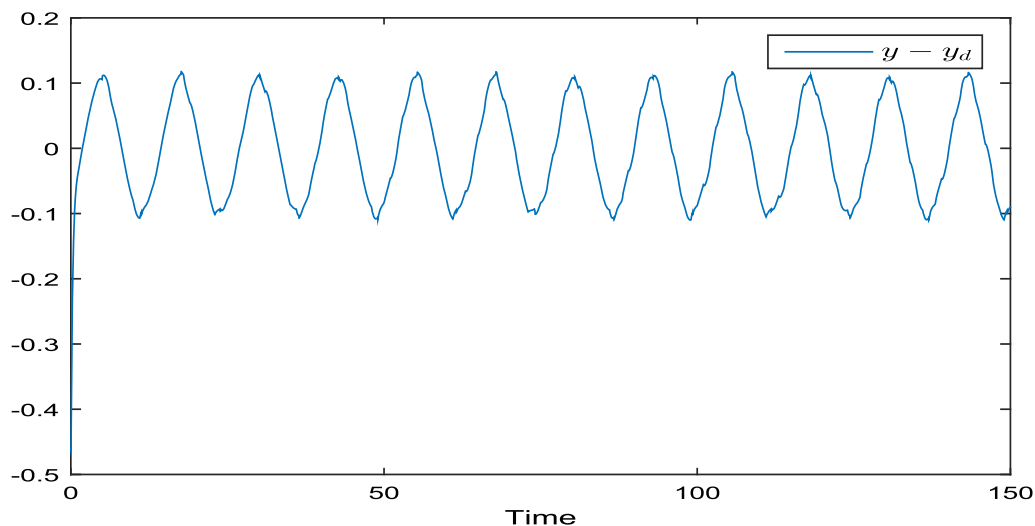


Fig. 11 Curve of tracking error $y - y_d$ for scheme 2 in Example 1

Remark 5 In [42, 43], the intelligent proportional-integral (iPI) controllers are proposed for flexible joint manipulator and the iPI controllers can obtain better disturbance and noise rejection performance. Compared with the proposed control scheme in this paper, some differences are listed as follows. First, the gains of the iPI controller in [42, 43] are constants while in this paper the gains of the proposed controller contains two parts: constant part and time-varying part. Second, the iPI controllers are designed for a second-system while in this paper we consider a n-order system and the generalized error is defined to derive the PI controller.

Remark 6 According to [52], we know the projection operator has two properties: (i) $\hat{\beta}_{\min} \leq \hat{\beta} \leq \hat{\beta}_{\max}$. (ii) $\tilde{\beta} \text{Proj}(\hat{\beta}, \Xi) \geq \tilde{\beta} \Xi$.

Next, the PI controller is designed using the backstepping method.

Step 1: The first-order derivative χ_1 is presented as

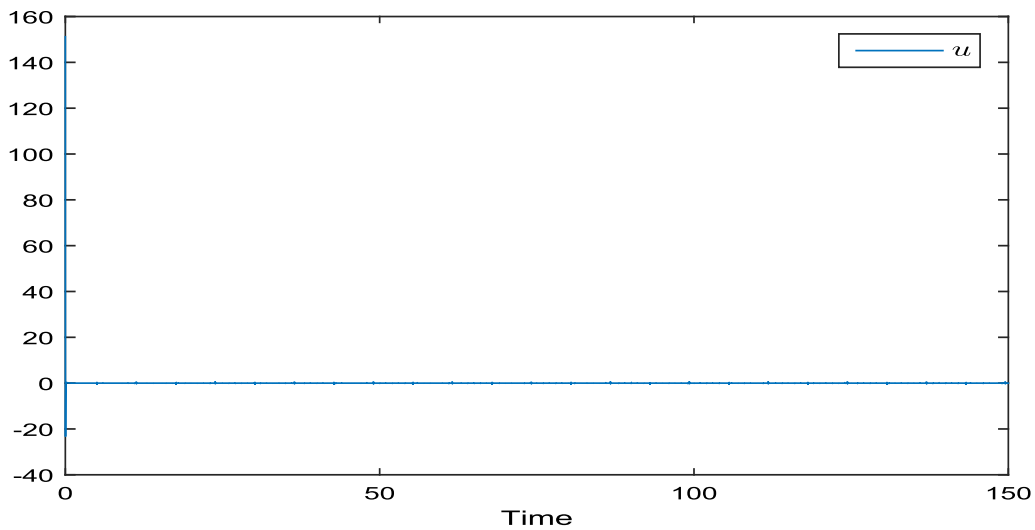


Fig. 12 Curve of control input u for scheme 2 in Example 1

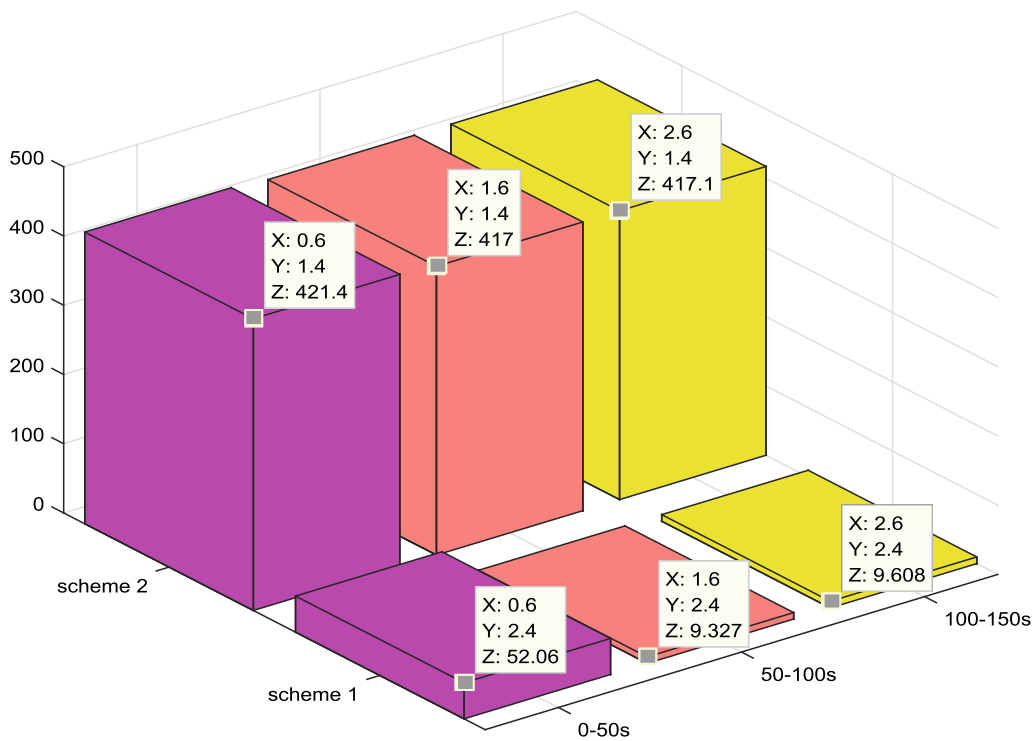


Fig. 13 Comparison of tracking performance between scheme 1 and scheme 2

$$\begin{aligned}
 \dot{\check{\chi}}_1 &= \dot{r}_1 + s_1 r_1 \\
 &= \dot{y} - \dot{y}_d + s_1 (y - y_d) \\
 &= \check{\beta} \dot{\check{\chi}}_1 - \dot{y}_d + s_1 (y - y_d) \\
 &= \check{\beta} (h \hat{\zeta}_2 + h w^* e_2 + f_{1,k}^* + \Delta_{1,k}^*) - \dot{y}_d + s_1 (y - y_d).
 \end{aligned}
 \tag{26}$$

Choose the Lyapunov function as

$$V_1 = \frac{1}{2} \check{\chi}_1^2.
 \tag{27}$$

Computing the derivative of V_1 leads to

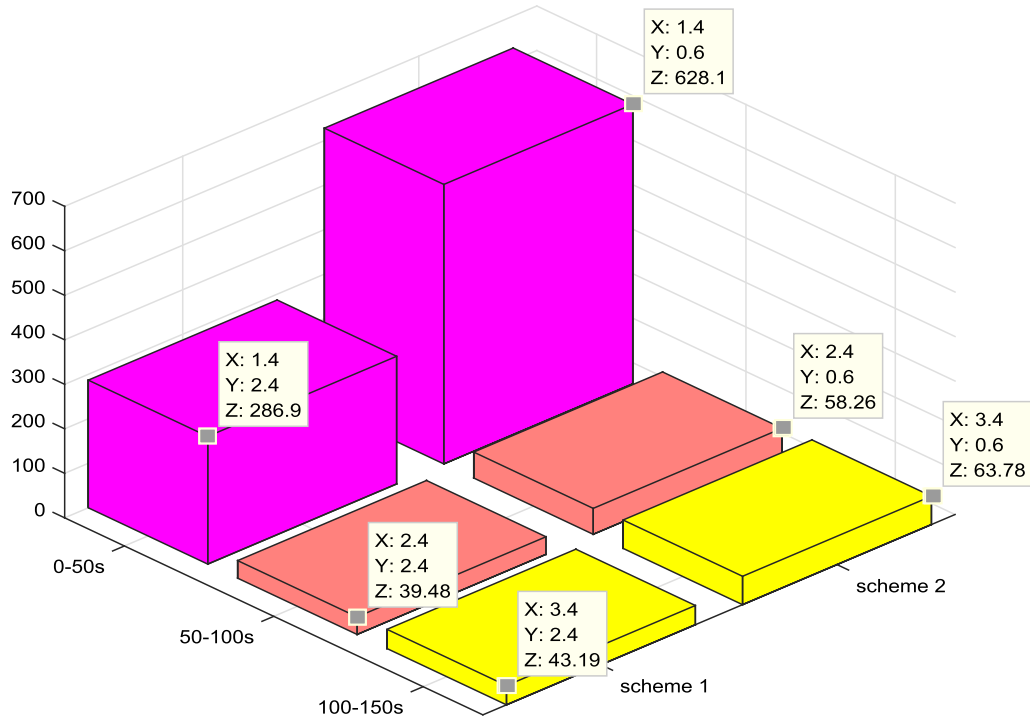


Fig. 14 Comparison of controlled quantity between scheme 1 and scheme 2

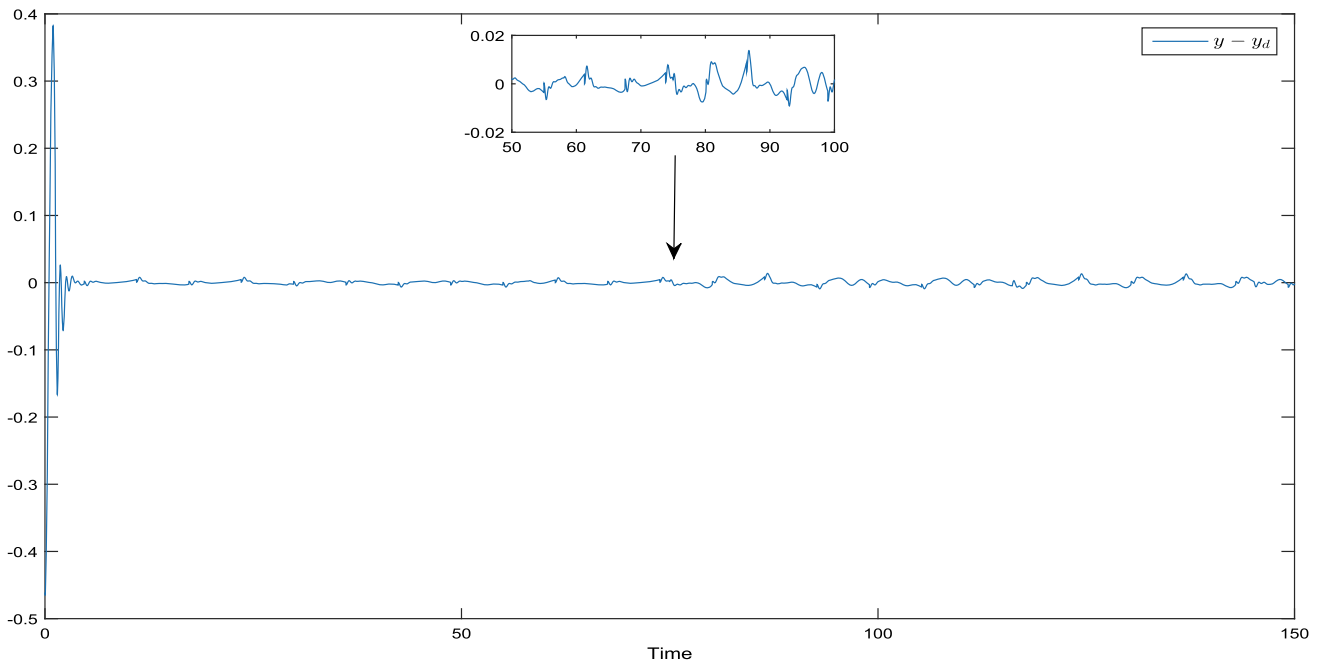


Fig. 15 Curve of the tracking error under the parameter perturbation

$$\begin{aligned} \dot{V}_1 &= \chi_1 \dot{\chi}_1 \\ &= \chi_1 (\check{\beta}(h\hat{\zeta}_2 + hw^*e_2 + f_{1,k}^* + \Delta_{1,k}^*) - \dot{y}_d + s_1(y - y_d)). \end{aligned} \tag{28}$$

To structure α_1 , the nonlinear function is defined as follows

$$\begin{aligned} \Psi_{1,k} &= \frac{\chi_1}{2} + \frac{1}{2}\chi_1 l^2 h^2 w^{*2} + \check{\beta} f_{1,k}^* + \frac{1}{4}l^2 \chi_1 w_{1k}^2 \\ &\quad + \check{\beta} w_{1k} \varphi_{12}(y) - \dot{y}_d + s_1(y - y_d) \\ &\quad - \check{\beta} h s_2 \int_0^t r_2 d\tau + \frac{2}{\chi_1} \tanh^2\left(\frac{\chi_1}{\varpi_1}\right) \eta_{1,k}(y), \end{aligned} \tag{29}$$

where $\eta_{1,k}(y) = b_k y^2 \bar{\varphi}_{12}^2(y)$.

Using FLSs, we have

$$\Psi_{1,k} = \Phi_{1,k}^T S_{1,k} + \vartheta_{1,k}, \tag{30}$$

where $\Phi_{1,k}$ denotes the weight of the FLSs $\Psi_{1,k}$, $S(X)_{1,k}$ is a basis function vector, and $\vartheta_{1,k}$ is a bounded function that satisfies $|\vartheta_{1,k}| \leq \varepsilon_{1,k}$, where $\varepsilon_{1,k}$ is a positive constant.

Then one has

$$\begin{aligned} \dot{V}_1 \leq & \chi_1 (\check{\beta} h \hat{\zeta}_2 + \Psi_{1,k} - \frac{\chi_1}{2} + \check{\beta} h w^* e_2 - \frac{1}{2} \chi_1 l^2 h^2 w^{*2} \\ & + \check{\beta} \Delta_{1,k}^* - \frac{1}{4} l^2 \chi_1 w_{1k}^2 - \check{\beta} w_{1k} \varphi_{12}(y) \\ & + \check{\beta} h s_2 \int_0^t r_2 d\tau - \frac{2}{\chi_1} \tanh^2 \left(\frac{\chi_1}{\varpi_1} \right) \eta_{1,k}(y)). \end{aligned} \tag{31}$$

Using Youngs inequality and Assumption 3 leads to

$$\chi_1 \check{\beta} h w^* e_2 \leq \frac{1}{2} \chi_1^2 l^2 h^2 w^{*2} + \frac{1}{2} e^T e, \tag{32}$$

$$\begin{aligned} \chi_1 \check{\beta} \Delta_{1,k}^* \leq & \chi_1 \check{\beta} w_{1k} \varphi_{11}(|\varsigma|) + \chi_1 \check{\beta} w_{1k} \varphi_{12}(y) \\ \leq & \frac{1}{4} \chi_1^2 l^2 w_{1k}^2 + \varphi_{11}^2(|\varsigma|) + \chi_1 \check{\beta} w_{1k} \varphi_{12}(y), \end{aligned} \tag{33}$$

Substituting (32) and (33) into (31), we have

$$\begin{aligned} \dot{V}_1 \leq & \chi_1 \check{\beta} h (\alpha_1 + \chi_2) + \chi_1 \Psi_{1,k} - \frac{\chi_1^2}{2} + \frac{1}{2} e^T e + \varphi_{11}^2(|\varsigma|) \\ & - 2 \tanh^2 \left(\frac{\chi_1}{\varpi_1} \right) \eta_{1,k}(y) \\ \leq & \chi_1 \check{\beta} h \alpha_1 + \check{\beta} h \chi_1 \chi_2 + \frac{\chi_1^2 \theta}{2 a_1^2} + \frac{a_1^2 + \varepsilon_{1,k}^2}{2} + \frac{1}{2} e^T e \\ & + \varphi_{11}^2(|\varsigma|) - 2 \tanh^2 \left(\frac{\chi_1}{\varpi_1} \right) \eta_{1,k}(y). \end{aligned} \tag{34}$$

Substituting the α_1 into (34) yields

$$\begin{aligned} \dot{V}_1 \leq & -\bar{\beta}_1 \chi_1^2 \hat{\beta} \left(c_1 + \frac{\hat{\theta}}{2 a_1^2} \right) + \check{\beta} h \chi_1 \chi_2 + \frac{\chi_1^2 \theta}{2 a_1^2} + \frac{a_1^2 + \varepsilon_{1,k}^2}{2} \\ & + \frac{1}{2} e^T e + \varphi_{11}^2(|\varsigma|) - 2 \tanh^2 \left(\frac{\chi_1}{\varpi_1} \right) \eta_{1,k}(y) \\ = & \frac{\tilde{\beta} \chi_1^2}{\beta} \left(c_1 + \frac{\hat{\theta}}{2 a_1^2} \right) + \frac{\chi_1^2 \tilde{\theta}}{2 a_1^2} + \frac{1}{2} e^T e + \varphi_{11}^2(|\varsigma|) - c_1 \chi_1^2 \\ & + \frac{a_1^2 + \varepsilon_{1,k}^2}{2} + \check{\beta} h \chi_1 \chi_2 \\ & - 2 \tanh^2 \left(\frac{\chi_1}{\varpi_1} \right) \eta_{1,k}(y). \end{aligned} \tag{35}$$

Step 2: By computing the derivative of χ_2 , we can obtain

$$\begin{aligned} \dot{\chi}_2 = & \dot{r}_2 + s_2 r_2 \\ = & \dot{\hat{\zeta}}_2 - \dot{\alpha}_1 + s_2 (\hat{\zeta}_2 - \alpha_1) \\ = & \hat{\zeta}_3 - \mu_{2,k} \hat{\zeta}_1 - \dot{\alpha}_1 + s_2 (\hat{\zeta}_2 - \alpha_1). \end{aligned} \tag{36}$$

Select Lyapunov function as

$$V_2 = V_1 + \frac{1}{2} \chi_2^2. \tag{37}$$

The derivative of V_2 is

$$\dot{V}_2 = \dot{V}_1 + \chi_2 (\hat{\zeta}_3 - \mu_{2,k} \hat{\zeta}_1 - \dot{\alpha}_1 + s_2 (\hat{\zeta}_2 - \alpha_1)). \tag{38}$$

The nonlinear function $\Psi_{2,k}$ is defined as

$$\begin{aligned} \Psi_{2,k} = & \frac{\chi_2}{2} - \mu_{2,k} \hat{\zeta}_1 - \dot{\alpha}_1 + s_2 (\hat{\zeta}_2 - \alpha_1) \\ & - s_3 \int_0^t r_3 d\tau + \check{\beta} h \chi_1 + \frac{2}{\chi_2} \tanh^2 \left(\frac{\chi_2}{\varpi_2} \right) \eta_{2,k}(y), \end{aligned} \tag{39}$$

where $\eta_{2,k}(y) = b_k y^2 \bar{\varphi}_{22}^2(y)$, which is estimated by FLSs

$$\Psi_{2,k} = \Phi_{2,k}^T S_{2,k} + \vartheta_{2,k}, \tag{40}$$

where $\Phi_{2,k}$ is weight of FLSs $\Psi_{2,k}$, $S(X)_{2,k}$ is a basis function vector, $\vartheta_{2,k}$ is a bounded function satisfies $|\vartheta_{2,k}| \leq \varepsilon_{2,k}$, $\varepsilon_{2,k}$ is a positive constant.

Similar to step 1, we have

$$\begin{aligned} \dot{V}_2 = & \dot{V}_1 + \chi_2 (\hat{\zeta}_3 - \mu_{2,k} \hat{\zeta}_1 - \dot{\alpha}_1 + s_2 (\hat{\zeta}_2 - \alpha_1)) \\ = & \dot{V}_1 + \chi_2 (\hat{\zeta}_3 + \Psi_{2,k} - \frac{\chi_2}{2} + s_3 \int_0^t r_3 d\tau - \check{\beta} h \chi_1 \\ & - \frac{2}{\chi_2} \tanh^2 \left(\frac{\chi_2}{\varpi_2} \right) \eta_{2,k}(y)) \\ \leq & \dot{V}_1 + \chi_2 \alpha_2 + \chi_2 \chi_3 + \frac{\chi_2^2 \theta}{2 a_2^2} + \frac{a_2^2 + \varepsilon_{2,k}^2}{2} - \check{\beta} h \chi_1 \chi_2 \\ & - 2 \tanh^2 \left(\frac{\chi_2}{\varpi_2} \right) \eta_{2,k}(y). \end{aligned} \tag{41}$$

Substituting α_2 into (41) leads to

$$\begin{aligned} \dot{V}_2 \leq & \dot{V}_1 + \chi_2 \chi_3 + \frac{\chi_2^2 \tilde{\theta}}{2 a_2^2} - c_2 \chi_2^2 + \frac{a_2^2 + \varepsilon_{2,k}^2}{2} - \check{\beta} h \chi_1 \chi_2 \\ & - 2 \tanh^2 \left(\frac{\chi_2}{\varpi_2} \right) \eta_{2,k}(y) \\ \leq & \frac{\tilde{\beta} \chi_1^2}{\beta} \left(c_1 + \frac{\hat{\theta}}{2 a_1^2} \right) + \frac{1}{2} e^T e + \varphi_{11}^2(|\varsigma|) + \chi_2 \chi_3 \\ & + \sum_{j=1}^2 \left\{ \frac{\chi_j^2 \tilde{\theta}}{2 a_j^2} - c_j \chi_j^2 + \frac{a_j^2 + \varepsilon_{j,k}^2}{2} - 2 \tanh^2 \left(\frac{\chi_j}{\varpi_j} \right) \eta_{j,k}(y) \right\}. \end{aligned} \tag{42}$$

Step $i(3 \leq i \leq n - 1)$: By calculating the derivative of χ_i , one has

$$\begin{aligned}\dot{\chi}_i &= \dot{r}_i + s_i r_i \\ &= \dot{\hat{\zeta}}_i - \dot{\alpha}_{i-1} + s_i(\hat{\zeta}_i - \alpha_{i-1}) \\ &= \hat{\zeta}_{i+1} - \mu_{i,k} \hat{\zeta}_1 - \dot{\alpha}_{i-1} + s_i(\hat{\zeta}_i - \alpha_{i-1}).\end{aligned}\quad (43)$$

Through the previous analysis, the derivative of V_{i-1} is expressed as:

$$\begin{aligned}\dot{V}_{i-1} &\leq \frac{\tilde{\beta} \chi_1^2}{\beta} \left(c_1 + \frac{\hat{\theta}}{2a_1^2} \right) + \frac{1}{2} e^T e + \varphi_{11}^2(|\varsigma|) + \chi_{i-1} \chi_i \\ &\quad + \sum_{j=1}^{i-1} \left\{ \frac{\chi_j^2 \tilde{\theta}}{2a_j^2} - c_j \chi_j^2 + \frac{a_j^2 + \varepsilon_{j,k}^2}{2} - 2 \tanh^2 \left(\frac{\chi_j}{\varpi_j} \right) \eta_{j,k}(y) \right\}.\end{aligned}\quad (44)$$

The Lyapunov function of step i can be selected as

$$V_i = V_{i-1} + \frac{1}{2} \chi_i^2. \quad (45)$$

The derivative of V_i is

$$\begin{aligned}\dot{V}_i &= \dot{V}_{i-1} + \chi_i \dot{\chi}_i \\ &= \dot{V}_{i-1} + \chi_i (\hat{\zeta}_{i+1} - \mu_{i,k} \hat{\zeta}_1 - \dot{\alpha}_{i-1} + s_i(\hat{\zeta}_i - \alpha_{i-1})).\end{aligned}\quad (46)$$

The nonlinear function $\Psi_{i,k}$ is defined as

$$\begin{aligned}\Psi_{i,k} &= \frac{\chi_i}{2} - \mu_{i,k} \hat{\zeta}_1 - \dot{\alpha}_{i-1} + s_i(\hat{\zeta}_i - \alpha_{i-1}) \\ &\quad - s_{i+1} \int_0^t r_{i+1} d\tau + \chi_{i-1} + \frac{2}{\chi_i} \tanh^2 \left(\frac{\chi_i}{\varpi_i} \right) \eta_{i,k}(y),\end{aligned}\quad (47)$$

where $\eta_{i,k}(y) = b_k y^2 \bar{\varphi}_{i,2}^2(y)$, which is estimated by FLSs

$$\Psi_{i,k} = \Phi_{i,k}^T S_{i,k} + \vartheta_{i,k}, \quad (48)$$

where $\Phi_{i,k}$ are the weights of the FLSs $\Psi_{i,k}$, $S(X)_{i,k}$ are basis function vectors, and $\vartheta_{i,k}$ is a bounded functions that satisfies $|\vartheta_{i,k}| \leq \varepsilon_{i,k}$, where $\varepsilon_{i,k}$ is a positive constant.

Then, we have

$$\begin{aligned}\dot{V}_i &= \dot{V}_{i-1} + \chi_i (\hat{\zeta}_{i+1} - \mu_{i,k} \hat{\zeta}_1 - \dot{\alpha}_{i-1} + s_i(\hat{\zeta}_i - \alpha_{i-1})) \\ &= \dot{V}_{i-1} + \chi_i (\hat{\zeta}_{i+1} + \Psi_{i,k} - \frac{\chi_i}{2} + s_{i+1} \int_0^t r_{i+1} d\tau \\ &\quad - \chi_{i-1} - \frac{2}{\chi_i} \tanh^2 \left(\frac{\chi_i}{\varpi_i} \right) \eta_{i,k}(y)) \\ &\leq \dot{V}_{i-1} + \chi_i \alpha_i + \chi_i \chi_{i+1} + \frac{\chi_i^2 \theta}{2a_i^2} + \frac{a_i^2 + \varepsilon_{i,k}^2}{2} - \chi_{i-1} \chi_i \\ &\quad - 2 \tanh^2 \left(\frac{\chi_i}{\varpi_i} \right) \eta_{i,k}(y).\end{aligned}\quad (49)$$

Substituting α_i into (49) gives

$$\begin{aligned}\dot{V}_i &\leq \frac{\tilde{\beta} \chi_1^2}{\beta} \left(c_1 + \frac{\hat{\theta}}{2a_1^2} \right) + \frac{1}{2} e^T e + \varphi_{11}^2(|\varsigma|) + \chi_{i-1} \chi_i \\ &\quad + \sum_{j=1}^{i-1} \left\{ \frac{\chi_j^2 \tilde{\theta}}{2a_j^2} - c_j \chi_j^2 + \frac{a_j^2 + \varepsilon_{j,k}^2}{2} - 2 \tanh^2 \left(\frac{\chi_j}{\varpi_j} \right) \eta_{j,k}(y) \right\} \\ &\quad + \chi_i \alpha_i + \chi_i \chi_{i+1} + \frac{\chi_i^2 \theta}{2a_i^2} + \frac{a_i^2 + \varepsilon_{i,k}^2}{2} - \chi_{i-1} \chi_i \\ &\quad - 2 \tanh^2 \left(\frac{\chi_i}{\varpi_i} \right) \eta_{i,k}(y) \\ &\leq \frac{\tilde{\beta} \chi_1^2}{\beta} \left(c_1 + \frac{\hat{\theta}}{2a_1^2} \right) + \frac{1}{2} e^T e + \varphi_{11}^2(|\varsigma|) + \chi_i \chi_{i+1} \\ &\quad + \sum_{j=1}^i \left\{ \frac{\chi_j^2 \tilde{\theta}}{2a_j^2} - c_j \chi_j^2 + \frac{a_j^2 + \varepsilon_{j,k}^2}{2} - 2 \tanh^2 \left(\frac{\chi_j}{\varpi_j} \right) \eta_{j,k}(y) \right\}.\end{aligned}\quad (50)$$

Step n : Calculating the derivative of χ_n gets

$$\begin{aligned}\dot{\chi}_n &= \dot{r}_n + s_n r_n \\ &= \dot{\hat{\zeta}}_n - \dot{\alpha}_{n-1} + s_n(\hat{\zeta}_n - \alpha_{n-1}) \\ &= u - \mu_{n,k} \hat{\zeta}_1 - \dot{\alpha}_{n-1} + s_n(\hat{\zeta}_n - \alpha_{n-1}).\end{aligned}\quad (51)$$

Select the Lyapunov function as

$$V_{n,k} = V_k^* + \bar{V} + V_{n-1} + \frac{1}{2} \chi_n^2 + \frac{1}{2j} \tilde{\theta}^2 + \frac{1}{2\beta} \tilde{\beta}^2, \quad (52)$$

where $\bar{V} = \int_0^{\varsigma} \rho(s) ds$ is a new function which is used to deal with state $\varsigma(t)$ and $\rho(s) > 0$ is a smooth decreasing function satisfying $\rho(0) = 0$.

Unknown function $\Psi_{n,k}$ in this step is defined as

$$\begin{aligned}\Psi_{n,k} &= \frac{\chi_n}{2} - \mu_{n,k} \hat{\zeta}_1 - \dot{\alpha}_{n-1} + s_n(\hat{\zeta}_n - \alpha_{n-1}) + \chi_{n-1} \\ &\quad + \frac{2}{\chi_n} \tanh^2 \left(\frac{\chi_n}{\varpi_n} \right) \eta_{n,k}(y),\end{aligned}\quad (53)$$

where $\eta_{n,k}(y) = b_k y^2 (\bar{\varphi}_{n,2}^2(y) + 1) + \rho(\frac{4n_0 \gamma(|y|)}{a_0}) n_0 \gamma(|y|)$. Bsing FLSs, one has

$$\Psi_{n,k} = \Phi_{n,k}^T S_{n,k} + \vartheta_{n,k}, \quad (54)$$

where $\Phi_{n,k}$ is the weight of the FLSs $\Psi_{n,k}$, $S(X)_{n,k}$ is a basis function vector, and $\vartheta_{n,k}$ is a bounded function that satisfies $|\vartheta_{n,k}| \leq \varepsilon_{n,k}$, where $\varepsilon_{n,k}$ is a positive constant.

The derivative of $V_{n,k}$ is calculated as

$$\begin{aligned}
 \dot{V}_{n,k} &= \dot{V}_k^* + \dot{V} + \dot{V}_{n-1} + \chi_n(u - \mu_{n,k}\hat{\varsigma}_1 - \dot{\alpha}_{n-1} \\
 &\quad + s_n(\hat{\varsigma}_n - \alpha_{n-1})) - \frac{1}{j}\tilde{\theta}\dot{\theta} - \frac{1}{\beta}\tilde{\beta}\dot{\beta} \\
 &= \dot{V}_k^* + \dot{V} + \dot{V}_{n-1} + \chi_n(u + \phi_{n,k} - \frac{\chi_n}{2} - \chi_{n-1} \\
 &\quad - \frac{2}{\chi_n}\tanh^2(\frac{\chi_n}{\varpi_n})\eta_{n,k}(y)) - \frac{1}{j}\tilde{\theta}\dot{\theta} - \frac{1}{\beta}\tilde{\beta}\dot{\beta} \\
 &\leq \dot{V}_k^* + \dot{V} + \dot{V}_{n-1} + \chi_n u + \frac{\chi_n^2\theta}{2a_n^2} + \frac{a_n^2 + \varepsilon_{n,k}^2}{2} \\
 &\quad - \chi_{n-1}\chi_n - 2\tanh^2\left(\frac{\chi_n}{\varpi_n}\right)\eta_{n,k}(y) - \frac{1}{j}\tilde{\theta}\dot{\theta} - \frac{1}{\beta}\tilde{\beta}\dot{\beta}.
 \end{aligned} \tag{55}$$

Substituting (18) (22) (24) (25) into (55) leads to

$$\begin{aligned}
 \dot{V}_{n,k} &\leq -e^T e + b_k y^2 \left(\sum_{i=1}^n \bar{\varphi}_{i,2}^2(y) + 1\right) \\
 &\quad + 8\|P_k\|^2 \sum_{i=1}^n \varphi_{i,1}^2(|\varsigma|) + d_{0,k} \\
 &\quad + \rho(V_\varsigma)[-a_0 V_\varsigma(\varsigma) + n_0 \gamma(|y|)] + \frac{1}{2}e^T e \\
 &\quad + \varphi_{11}^2(|\varsigma|) + \sum_{i=1}^n \left\{ -c_i \chi_i^2 \right. \\
 &\quad \left. + \frac{a_i^2 + \varepsilon_{i,k}^2}{2} - 2\tanh^2\left(\frac{\chi_i}{\varpi_i}\right)\eta_{i,k}(y) \right\} + \frac{\hbar}{j}\tilde{\theta}\dot{\theta} + \frac{l}{\beta}\tilde{\beta}\dot{\beta}.
 \end{aligned} \tag{56}$$

Note that $\bar{V} = \int_0^{V_\varsigma} \rho(s)ds \leq V_\varsigma(\varsigma)\rho(V_\varsigma(\varsigma))$. The following inequality holds

$$\begin{aligned}
 &\rho(V_\varsigma)[-a_0 V_\varsigma(\varsigma) + n_0 \gamma(|y|)] \\
 &= -a_0 \rho(V_\varsigma)V_\varsigma(\varsigma) + \rho(V_\varsigma)n_0 \gamma(|y|) \\
 &= -\frac{1}{2}a_0 \bar{V} - \frac{1}{4}a_0 \rho(V_\varsigma)V_\varsigma(\varsigma) \\
 &\quad - \frac{1}{4}a_0 \rho(V_\varsigma)V_\varsigma(\varsigma) + \rho(V_\varsigma)n_0 \gamma(|y|).
 \end{aligned} \tag{57}$$

Case 1 $n_0 \gamma(|y|) < \frac{1}{4}a_0 V_\varsigma(\varsigma)$. We have

$$\begin{aligned}
 &\rho(V_\varsigma)[-a_0 V_\varsigma(\varsigma) + n_0 \gamma(|y|)] \\
 &\leq -\frac{1}{2}a_0 \bar{V} - \frac{1}{4}a_0 \rho(V_\varsigma)V_\varsigma(\varsigma).
 \end{aligned} \tag{58}$$

Case 2 $n_0 \gamma(|y|) \geq \frac{1}{4}a_0 V_\varsigma(\varsigma)$. Then $V_\varsigma(\varsigma) \leq \frac{4n_0 \gamma(|y|)}{a_0}$, one has

$$\begin{aligned}
 &\rho(V_\varsigma)[-a_0 V_\varsigma(\varsigma) + n_0 \gamma(|y|)] \\
 &\leq -\frac{1}{2}a_0 \bar{V} - \frac{1}{4}a_0 \rho(V_\varsigma)V_\varsigma(\varsigma) + \rho\left(\frac{4n_0 \gamma(|y|)}{a_0}\right)n_0 \gamma(|y|).
 \end{aligned} \tag{59}$$

By combining (58) with (59), (56) can be transformed as

$$\begin{aligned}
 \dot{V}_{n,k} &\leq -e^T e + b_k y^2 \left(\sum_{i=1}^n \bar{\varphi}_{i,2}^2(y) + 1\right) \\
 &\quad + 8\|P_k\|^2 \sum_{i=1}^n \varphi_{i,1}^2(|\varsigma|) + d_{0,k} - \frac{1}{2}a_0 \bar{V} \\
 &\quad - \frac{1}{4}a_0 \rho(V_\varsigma)V_\varsigma(\varsigma) + \rho\left(\frac{4n_0 \gamma(|y|)}{a_0}\right)n_0 \gamma(|y|) \\
 &\quad + \frac{1}{2}e^T e + \varphi_{11}^2(|\varsigma|) + \sum_{i=1}^n \left\{ -c_i \chi_i^2 \right. \\
 &\quad \left. + \frac{a_i^2 + \varepsilon_{i,k}^2}{2} - 2\tanh^2\left(\frac{\chi_i}{\varpi_i}\right)\eta_{i,k}(y) \right\} + \frac{\hbar}{j}\tilde{\theta}\dot{\theta} + \frac{l}{\beta}\tilde{\beta}\dot{\beta}.
 \end{aligned} \tag{60}$$

Choose the appropriate function ρ such that

$$8\|P_k\|^2 \sum_{i=1}^n \varphi_{i,1}^2(|\varsigma|) + \varphi_{11}^2(|\varsigma|) \leq \frac{1}{4}a_0 \rho(V_\varsigma)V_\varsigma(\varsigma). \tag{61}$$

Notice that the following inequalities hold

$$\begin{aligned}
 \tilde{\theta}\dot{\theta} &= \tilde{\theta}(\theta - \tilde{\theta}) \leq -\frac{1}{2}\tilde{\theta}^2 + \frac{1}{2}\theta^2, \\
 \tilde{\beta}\dot{\beta} &= \tilde{\beta}(\beta - \tilde{\beta}) \leq -\frac{1}{2}\tilde{\beta}^2 + \frac{1}{2}\beta^2.
 \end{aligned} \tag{62}$$

Then we have

$$\begin{aligned}
 \dot{V}_{n,k} &\leq -p_1 V_{n,k} + p_2 + \eta_k(y) + \sum_{i=1}^n \left\{ -2\tanh^2\left(\frac{\chi_i}{\varpi_i}\right)\eta_{i,k}(y) \right\} \\
 &= -p_1 V_{n,k} + p_2 + \sum_{i=1}^n \left\{ \left(1 - 2\tanh^2\left(\frac{\chi_i}{\varpi_i}\right)\right)\eta_{i,k}(y) \right\}.
 \end{aligned} \tag{63}$$

where $p_1 = \min\{\frac{1}{2\lambda_{\max}(P_k)}, 2c_i, \hbar, l, \frac{1}{2}a_0\}$, $p_2 = \max\{d_{0,k} + \frac{a_i^2 + \varepsilon_{i,k}^2}{2} + \frac{\hbar}{2j}\theta^2 + \frac{l}{2}\beta^2\}$, $\eta_k(y) = \eta_{1,k}(y) + \eta_{2,k}(y) + \dots + \eta_{n,k}(y) = \sum_{i=1}^n b_k y^2 (\sum_{i=1}^n \bar{\varphi}_{i,2}^2(y) + 1) + \rho(\frac{4n_0 \gamma(|y|)}{a_0})n_0 \gamma(|y|)$.

Remark 7 The controller designed in this paper has a PI form that features a simple structure and a more explicit physical meaning. To achieve the above objectives, the generalized errors are introduced, and the nonlinear functions $\Psi_{i,k}$ are intelligently constructed in each step. These functions can be approximated via FLSs because of their continuity.

Remark 8 The polynomial $\frac{1}{2}\chi_1 l^2 h^2 w^{*2} + \frac{1}{4}l^2 \chi_1 w_{1k}^2 + \check{\beta} w_{1k} \varphi_{12}(y)$ is introduced in $\Psi_{1,k}$ to counteract the nonlinear functions $\frac{1}{2}\chi_1^2 l^2 h^2 w^{*2}$, $\frac{1}{4}l^2 \chi_1^2 w_{1k}^2$ and $\chi_1 \check{\beta} w_{1k} \varphi_{12}(y)$ produced in (32) and (33).

Remark 9 The function $\frac{\chi_i}{2}$ is introduced in $\Psi_{i,k}$ to counteract the function $\frac{\chi_i^2}{2}$ produced $\chi_i \vartheta_{i,k} \leq \frac{\chi_i}{2} + \frac{\varepsilon_{i,k}^2}{2}$; in order to construct the virtual control laws with a PI structure and

deal with the function $\eta_k(y)$, the polynomial $-s_{i+1} \int_0^t r_{i+1} d\tau + \frac{2}{\chi_i} \tanh^2(\frac{\chi_i}{\varpi_i}) \eta_{i,k}(y)$ is introduced.

Remark 10 To estimate the nonlinear term $\eta_k(y)$, the function $\tanh^2(\frac{\chi_i}{\varpi_i})$ is introduced because of $\lim_{\chi_i \rightarrow 0} \frac{\tanh^2(\frac{\chi_i}{\varpi_i})}{\chi_i} = 0$, thus, it can be reconstructed using FLSs. As a result, the difficulty caused by the existence of the nonlinear function $\eta_k(y)$ is solved.

3.3 Stability Analysis

Theorem 1 Consider an uncertain switched nonlinear system (1) with Assumptions 1–3 and an average dwell time $\tau_a > \frac{\ln \mu}{p_1} (\mu = \max\{\frac{\lambda_{\max}(P_k)}{\lambda_{\min}(P_l)}\}, k, l \in \mathcal{P}; p_1 = \min\{\frac{1}{2\lambda_{\max}(P_k)}, 2c_i, \hat{h}, t, \frac{1}{2}a_0\})$, the PI controller (22) and the adaptive laws (24)–(25) can guarantee that all the signals in the closed-loop system and tracking error are bounded.

Proof We will discuss the stability of the system in three cases.

Case 1 If $\chi_i \notin \mathcal{E}_{\chi_i}, i = 1, 2, \dots, n$, by applying Lemma 2, (63) is rewritten as

$$\begin{aligned} \dot{V}_{n,k} &\leq -p_1 V_{n,k} + p_2 + \sum_{i=1}^n \left\{ \left(1 - 2 \tanh^2 \left(\frac{\chi_i}{\varpi_i} \right) \right) \eta_{i,k}(y) \right\} \\ &\leq -p_1 V_{n,k} + p_2. \end{aligned} \tag{64}$$

Integrating both sides of (64) on $[t_j, t_{j+1})$ yields

$$V_{n,k}(t) \leq e^{-p_1(t-t_j)} V_{n,k}(t_j) + p_2 \int_{t_j}^t e^{-p_1(t-s)} ds, \tag{65}$$

where t_j denotes switching time, $j = 0, 1, \dots, N_\sigma(t, 0) - 1$. We know that $\mathcal{V}_{n,k} \leq \mu \mathcal{V}_{n,l}$ in [53], where $k, l \in \mathcal{P}$, and $\mu = \max\{\frac{\lambda_{\max}(P_k)}{\lambda_{\min}(P_l)}\} \geq 1$.

Let $t_0 = 0$. For any $t > 0$, iterating the (65) leads to

$$\begin{aligned} V_{n,k}(t) &\leq e^{-p_1(t-t_{N_\sigma(t,0)})} V_{n,k}(t_{N_\sigma(t,0)}) + p_2 \int_{t_{N_\sigma(t,0)}}^t e^{-p_1(t-s)} ds \\ &\leq \mu e^{-p_1(t-t_{N_\sigma(t,0)})} V_{n,\sigma}(t_{N_\sigma(t,0)}) + p_2 \int_{t_{N_\sigma(t,0)}}^t e^{-p_1(t-s)} ds \\ &\leq \mu e^{-p_1(t-t_{N_\sigma(t,0)})} [e^{-p_1(t_{N_\sigma(t,0)}-t_{N_\sigma(t,0)-1})} V(t_{N_\sigma(t,0)-1}) \\ &\quad + p_2 \int_{t_{N_\sigma(t,0)-1}}^{t_{N_\sigma(t,0)}} e^{-p_1(t_{N_\sigma(t,0)}-s)} ds] + p_2 \int_{t_{N_\sigma(t,0)}}^t e^{-p_1(t-s)} ds \\ &\leq \dots \\ &\leq \mu^{N_\sigma(t,0)} e^{-p_1 t} V_{n,\sigma(0)}(0) + p_2 \int_0^t \mu^{N_\sigma(t,s)} e^{-p_1(t-s)} ds. \end{aligned} \tag{66}$$

Choose $\tau_a > \frac{\ln \mu}{p_1}$. According to the definition of the average dwell time [53, 54] and for arbitrary $\gamma \in (0, p_1 - \frac{\ln \mu}{\tau_a})$, we have

$$N_\sigma(t, 0) \leq N_0 + \frac{(p_1 - \gamma)t}{\ln \mu}. \tag{67}$$

Taking (67) into (66) yields

$$\begin{aligned} V_{n,\sigma}(t) &\leq \mu^{N_0 + \frac{(p_1 - \gamma)t}{\ln \mu}} e^{-p_1 t} \mathcal{V}_{\sigma(0)}(0) \\ &\quad + p_2 \int_0^t \mu^{N_0 + \frac{(p_1 - \gamma)(t-s)}{\ln \mu}} e^{-p_1(t-s)} ds \\ &= \mu^{N_0} e^{(p_1 - \gamma)t} e^{-p_1 t} V_{\sigma(0)}(0) \\ &\quad + \mu^{N_0} p_2 \int_0^t e^{(p_1 - \gamma)(t-s)} e^{-p_1(t-s)} ds \\ &= \mu^{N_0} e^{-\gamma t} V_{\sigma(0)}(0) + \mu^{N_0} \frac{p_2}{\gamma} (1 - e^{-\gamma t}). \end{aligned} \tag{68}$$

Thus, we can obtain $V_{n,\sigma}(t) \leq \mu^{N_0} \frac{p_2}{\gamma}$ when $t \rightarrow \infty$. Therefore, e_i, χ_i and $\tilde{\theta}, i = 1, 2, \dots, n$ are bounded; then, $\alpha_1, \alpha_2, \dots, \alpha_{n-1}, u, \hat{\theta}, \hat{\beta}$ are bounded. Then we can further obtain $r_i, \tilde{\zeta}_i, \hat{\zeta}_i, \zeta_i, y, \varsigma$, and x_i are bounded.

According to the above analysis, the following inequality holds

$$\frac{1}{2} \chi_1^2 \leq \mu^{N_0} \frac{p_2}{\gamma}, \tag{69}$$

so

$$|\chi_1| \leq \sqrt{2\mu^{N_0} \frac{p_2}{\gamma}}. \tag{70}$$

Note that

$$\chi_1 = r_1 + s_1 \int_0^t r_1 d\tau. \tag{71}$$

Let $p = \int_0^t r_1 d\tau$. We have

$$\chi_1 = \dot{p} + s_1 p. \tag{72}$$

Furthermore, we obtain

$$-\sqrt{2\mu^{N_0} \frac{p_2}{\gamma}} \leq \dot{p} + s_1 p \leq \sqrt{2\mu^{N_0} \frac{p_2}{\gamma}}. \tag{73}$$

Multiplying both sides by $\exp(s_1 t)$ produces

$$-\exp(s_1 t) \sqrt{2\mu^{N_0} \frac{p_2}{\gamma}} \leq \frac{d(p \exp(s_1 t))}{dt} \leq \exp(s_1 t) \sqrt{2\mu^{N_0} \frac{p_2}{\gamma}}. \tag{74}$$

Integrating (74) leads to

$$\begin{aligned}
 & -\frac{\sqrt{2\mu^{N_0} p_2}}{s_1} + \left[p(0) + \frac{\sqrt{2\mu^{N_0} p_2}}{s_1} \right] \exp(-s_1 t) \leq p \\
 & \leq \frac{\sqrt{2\mu^{N_0} p_2}}{s_1} + \left[p(0) - \frac{\sqrt{2\mu^{N_0} p_2}}{s_1} \right] \exp(-s_1 t).
 \end{aligned} \tag{75}$$

Thus we have

$$|p| \leq \frac{\sqrt{2\mu^{N_0} p_2}}{s_1}. \tag{76}$$

Combining (72) with (76) gives

$$\lim_{t \rightarrow \infty} |y - y_d| = |r_1| \leq 2\sqrt{2\mu^{N_0} \frac{p_2}{\gamma}}. \tag{77}$$

Case 2 If $\chi_i \in \mathcal{E}_{\chi_i}$, $i = 1, 2, \dots, n$, thus $|\chi_i| \leq \iota\varpi_i$ is bounded. Furthermore, from the choice of the adaptive laws $\hat{\theta}$ in (23), we can infer that $\hat{\theta}$ is bounded for any bounded χ_i , which means that $\tilde{\theta}$ is also bounded. Similar to Case 1, $\alpha_1, \alpha_2, \dots, \alpha_{n-1}, u, r_i, \varsigma, \hat{\zeta}$ and y are bounded, and given that $\bar{\varphi}_{i,2}(y)$ and $\varphi_{i,1}(|\varsigma|)$ are smooth functions, then $\bar{\varphi}_{i,2}(y)$ and $\varphi_{i,1}(|\varsigma|)$ are bounded, and $\tilde{\zeta}_i, \zeta_i$ and x_i are bounded when τ_a satisfies $\tau_a > \frac{\ln \mu}{p_1}$. There exist some positive constants M_i , such that $\max_{k \in \mathcal{P}} \{\eta_{i,k}\} \leq M_i$, and we can further obtain $(1 - 2 \tanh^2(\frac{\chi_i}{\varpi_i}))\eta_{i,k} \leq 3M_i$. Then (63) can be written as

$$\dot{V}_{n,k} \leq \bar{p}_2 - p_1 V_{n,k}, \tag{78}$$

where $\bar{p}_2 = p_2 + 3 \sum_{i=1}^n M_i$.

Similar to Case 1, we can get

$$\lim_{t \rightarrow \infty} |y - y_d| = |r_1| \leq 2\iota\varpi_1. \tag{79}$$

Case 3. If $\chi_j \notin \mathcal{E}_{\chi_j}$ and $\chi_i \in E_{\chi_i}$, $i \neq j$. (63) can be rewritten as

$$\begin{aligned}
 \dot{V}_{n,k} & \leq -p_1 V_{n,k} + p_2 + \sum_{i=1}^n \left\{ \left(1 - 2 \tanh^2 \left(\frac{\chi_i}{\varpi_i} \right) \right) \eta_{i,k}(y) \right\}. \\
 & = -p_1 V_{n,k} + p_2 + \sum_{\chi_j \notin E_{\chi_j}} \left\{ \left(1 - 2 \tanh^2 \left(\frac{\chi_j}{\varpi_j} \right) \right) \eta_{j,k}(y) \right\} \\
 & \quad + \sum_{\chi_i \in E_{\chi_i}} \left\{ \left(1 - 2 \tanh^2 \left(\frac{\chi_i}{\varpi_i} \right) \right) \eta_{i,k}(y) \right\}.
 \end{aligned} \tag{80}$$

Combining Case 1 with Case 2 yields

$$\lim_{t \rightarrow \infty} |y - y_d| \leq \max \left\{ 2\sqrt{2\mu^{N_0} \frac{p_2}{\gamma}}, 2\iota\varpi_1 \right\}. \tag{81}$$

Based on the discussed above, Theorem 1 is proved.

The specific implementation steps are summarized as follows:

1. Choose the appropriate parameters $\mu_{i,k}$ such that A_k is a Hurwitz matrix, $i = 1, 2, \dots, n$.
2. Calculate the corresponding P_k through (13).
3. Select the positive constants h, j, c_1, ι and a_i to determine the adaptive law $\hat{\theta}, \hat{\beta}$.
4. Choose the parameters $c_i > 0, s_i > 0$ to determine the virtual control functions $\alpha_i, i = 1, 2, \dots, n - 1$.
5. Select the parameters $c_n > 0, s_n > 0$ to determine the controller u .
6. Choose the average dwell time τ_a by calculating $\frac{\ln \mu}{p_1}$.

Remark 9 According to (81), to achieve a good control performance, we can add the value of γ and reduce the value of p_2 by adjusting the correlative parameters. However, this adjustment may also influence other performance aspects such as the resulting large controlled quantity. Thus, a specific control performance and control action are achieved via regulation parameters.

4 Simulation Results

In this section, two examples are given to demonstrate the effectiveness of the developed method.

Example 1 Consider the following switched nonlinear systems with unmodeled dynamics:

$$\begin{aligned}
 \dot{\varsigma} & = q_{\sigma(t)}(\varsigma, y, d(t)), \\
 \dot{x}_1 & = h_1 x_2 + f_{1,\sigma(t)}(x_1) + \Delta_{1,\sigma(t)}(\varsigma, y, d(t)), \\
 \dot{x}_2 & = h_2 x_3 + f_{2,\sigma(t)}(x_1, x_2) + \Delta_{2,\sigma(t)}(\varsigma, y, d(t)), \\
 \dot{x}_n & = h_3 u + f_{3,\sigma(t)}(x_1, x_2, x_3) + \Delta_{3,\sigma(t)}(\varsigma, y, d(t)), \\
 y & = D(x_1),
 \end{aligned} \tag{82}$$

where $q_1 = -\varsigma + 0.125y^2 \cos^2(y)$, $q_2 = -2\varsigma + 0.05y^2 \sin^2(y)$, $f_{1,1} = 0.1 \sin(x_1)$, $f_{1,2} = 0.1 \cos(x_1)$, $f_{2,1} = 0.1 \sin(x_1 x_2)$, $f_{2,2} = 0.1 \sin(x_1) \cos(x_2)$, $f_{3,1} = 0.1 \cos(x_1^2 x_2 x_3)$, $f_{3,2} = 0.1 \sin(x_1 x_2) \cos(x_3)$, $\Delta_{1,1} = 0.1 \sin(y\varsigma) + 0.1e^{-t^2}$, $\Delta_{1,2} = 0.1 \cos(y\varsigma) - 0.1e^{-t^2}$, $\Delta_{2,1} = 0.1 \sin(y\varsigma) + 0.2 \sin(t^2)$, $\Delta_{2,2} = 0.1 \sin(y^2\varsigma) + 0.2 \cos(t^4)$, $\Delta_{3,1} = 0.1 \sin(y\varsigma) + e^{-t^4}$, $\Delta_{3,2} = 0.1 \cos(y\varsigma) + 0.5e^{-t^2}$. We choose the tracking signal as $y_d = 0.5 \cos(0.5t) + \sin(0.5t)$. Choose $\mu_{1,1} = \mu_{1,2} = 3$, $\mu_{2,1} = \mu_{2,2} = 5$, $\mu_{3,1} = \mu_{3,2} = 2$, $\tau_a = 29.03 > \ln 13.8392/0.0905$. choose the initial conditions $x_1(0) = 0.2$, $x_2(0) = 0.3$, $x_3(0) = -0.2$, $\hat{\zeta}_1(0) = \hat{\zeta}_2(0) = \hat{\zeta}_3(0) = 0$, $\hat{\theta}(0) = 0$, $\hat{\beta}(0) = 0.03$. Select the parameters as: $l = 0.2$, $v = 0.01$, $j_1 = 2.5$, $h = 0.1$, $\iota = 0.001$, $a_1 = 2$, $a_2 = 1$, $a_3 = 3$, $s_1 = s_2 = s_3 = 2$, $c_1 = 2$, $c_2 = 7$, $c_3 = 100$, $h_1 = 1$, $h_2 = 3$, $h_3 = 70$. The simulation results are shown in Figs. 2, 3, 4, 5, 6, 7, 8, and 9. Figure 2 gives the trajectories of y and y_d whereas Fig. 3

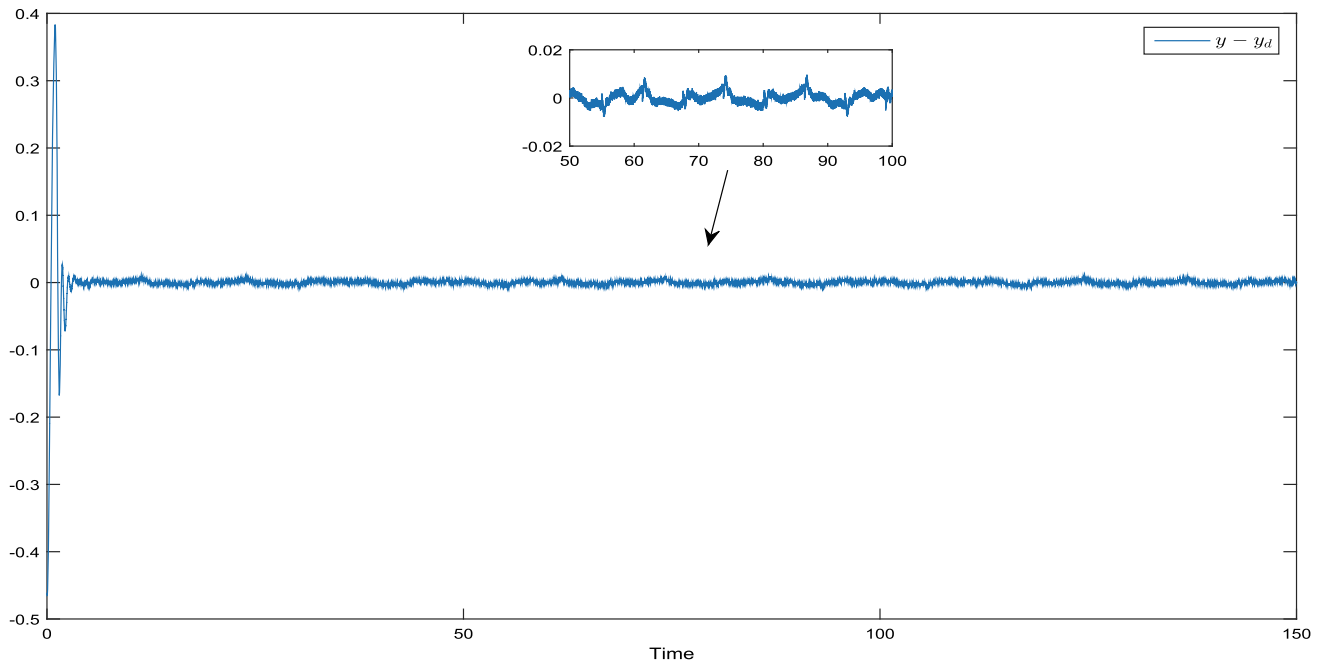


Fig. 16 Curve of tracking error with noise

shows the curve of tracking error. From Figs. 2 and 3, we can distinctly observe that the system has a good tracking performance. Figure 4 presents the curves of x_1 , x_2 , x_3 and ς . Curves of $\hat{\zeta}_1$, $\hat{\zeta}_2$, and $\hat{\zeta}_3$ are shown in Fig. 5. Figures 6 and 7 depict curves of the adaptive parameters $\hat{\theta}$ and $\hat{\beta}$, respectively. Figure 8 shows curve of the control input u . Figure 9 depicts the switching signal. To prove the superiority of the proposed scheme, we compare the simulation results with [55]. For convenience, the scheme proposed in this paper is denoted as scheme 1, whereas the scheme proposed in [55] is denoted as scheme 2. To ensure a fair comparison, we choose the same q_k , $f_{i,k}$, $\Delta_{i,k}$, and h_i . The simulation results for scheme 2 are shown in Figs. 10, 11, and 12. Figure 10 shows curves of the y and y_d . Curve of tracking error is presented in Fig. 10, and 12 depicts the trajectories of u . Figures 13 and 14 show the comparison of tracking performance and control quantity between scheme 1 and scheme 2. It can be observed that scheme 1 has better tracking performance than scheme 2 provided that the two control quantities are close to each other.

In order to verify the robustness of the proposed scheme, we choose the nonlinear functions as $f_{1,1} = 0.1 \sin(x_1)$, $f_{1,2} = 0.1 \cos(x_1)$, $f_{2,1} = 0.1 \sin(x_1 x_2)$, $f_{2,2} = 0.1 \sin(x_1) \cos(x_2)$, $f_{3,1} = 0.1 \cos(x_1^2 x_2 x_3)$, $f_{3,2} = 0.1 \sin(x_1 x_2) \cos(x_3)$ when $t < 75s$; while $t \geq 75s$, the nonlinear functions are selected as $f_{1,1} = 0.3 \sin(x_1)$, $f_{1,2} = 0.3 \cos(x_1)$, $f_{2,1} = 0.3 \sin(x_1 x_2)$, $f_{2,2} = 0.3 \sin(x_1) \cos(x_2)$, $f_{3,1} = 0.3 \cos(x_1^2 x_2 x_3)$, $f_{3,2} = 0.3 \sin(x_1 x_2) \cos(x_3)$. The tracking performance under parameter perturbation is shown in Fig. 15, which demonstrates that the proposed scheme has a

significant robustness. Finally, we investigate the noise rejection performance of the system. A noise with an SNR of 60 dB is added to the output channel (82). Curves of system tracking error with sensor noise is depicted in Fig. 16. Curve of the input u is shown in Fig. 17. It can be clearly observed that the tracking error has a satisfactory performance when the systems are subject to sensor noise.

Example 2 (Electromechanical system). An electromechanical system [56] can be modeled as follows

$$\begin{aligned} P\ddot{z} + M\dot{z} + Q \sin(z) &= I \\ LI &= U_\epsilon - RI - K_B \dot{z}, \end{aligned} \quad (83)$$

where $P = \frac{N}{K_\tau} + \frac{m_0 l^2}{3K_\tau} + \frac{m_1 l^2}{K_\tau} + \frac{2m_1 R_0^2}{5K_\tau}$, $Q = \frac{m_0 l G}{2K_\tau} + \frac{m_1 l G}{K_\tau}$, $M = \frac{D_0}{K_\tau}$, z is angular motor position, I represents motor armature current, $L = 1.429 \times 10^{-2} H$ denotes armature inductance, U_ϵ means the input control voltage, $R = 1 \times 10^{-2} \Omega$ is called armature resistance, $K_B = 2 \times 10^{-3} Nm/A$ is back-emf coefficient, $K_\tau = 0.9 Nm/A$ is a coefficient which means the electromechanical conversion of armature current to torque, $N = 16.25 \times 10^{-2} kgm^2$ represents the rotor inertia, $m_0 = 5.06 \times 10^{-2} kg$ and $m_1 = 4.34 \times 10^{-2} kg$ denote link mass and load mass, respectively. $l = 5 \times 10^{-2} m$ is the link length, $R_0 = 2.3 \times 10^{-2} m$ is called radius of the load, $G = 9.8 m/s^2$ represents the gravity coefficient, and $D_0 = 1.625 \times 10^{-3} Nms/rad$ represents the coefficient of viscous friction at the joint. Let $x_1 = z$, $x_2 = \dot{z}$, $x_3 = \frac{l}{P}$, $u = U_\epsilon$. Considering the

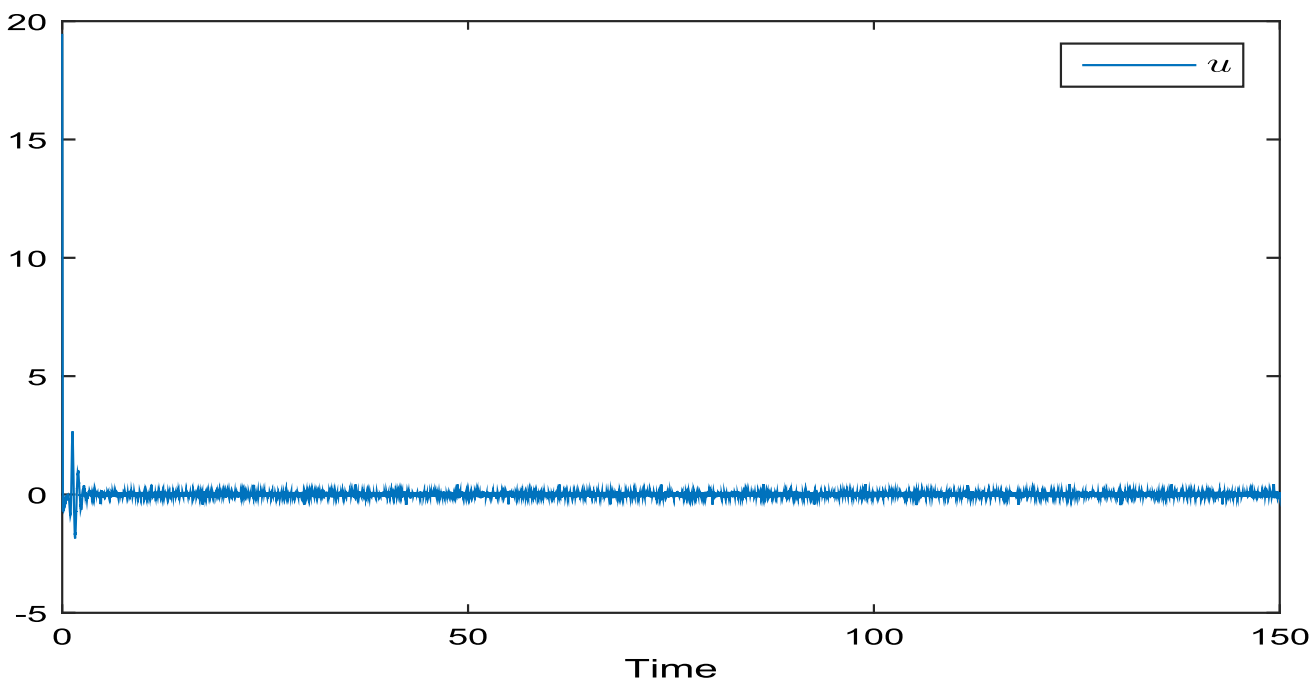


Fig. 17 Curve of controller u with noise

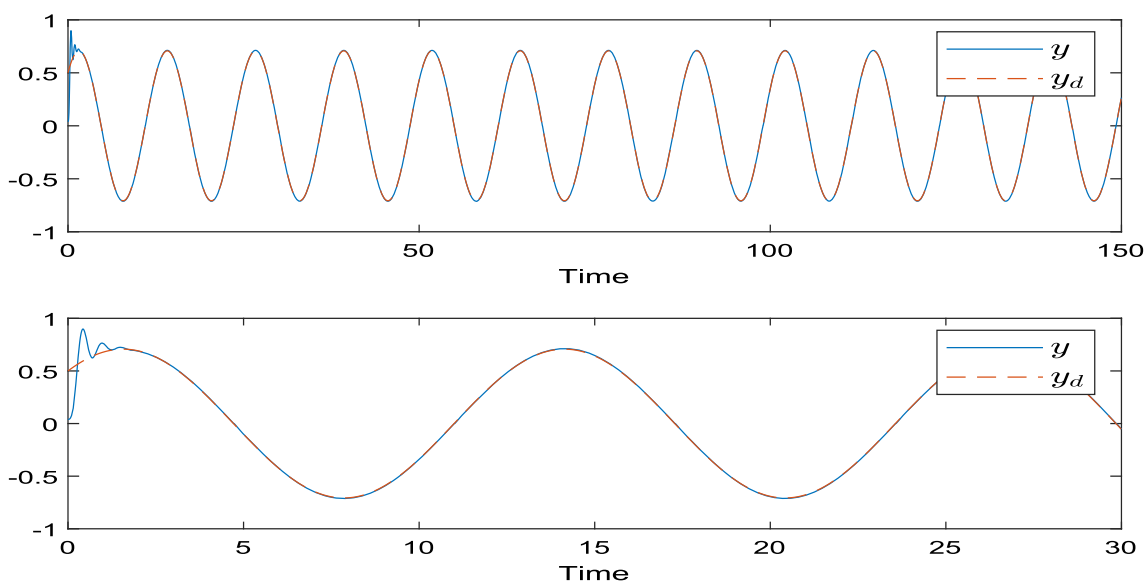


Fig. 18 Curves of y and y_d for Example 2

disturbances, unmodeled dynamics and dead-zone output, the system (83) can be expressed as

$$\begin{aligned}
 \dot{\zeta} &= q_{\sigma(t)}(\zeta, y, d(t)), \\
 \dot{x}_1 &= h_1 x_2 + f_{1,\sigma(t)}(x_1) + \Delta_{1,\sigma(t)}(\zeta, y, d(t)), \\
 \dot{x}_2 &= h_2 x_3 + f_{2,\sigma(t)}(x_1, x_2) + \Delta_{2,\sigma(t)}(\zeta, y, d(t)), \\
 \dot{x}_n &= h_3 u + f_{3,\sigma(t)}(x_1, x_2, x_3) + \Delta_{3,\sigma(t)}(\zeta, y, d(t)), \\
 y &= D(x_1),
 \end{aligned} \tag{84}$$

where $q_1 = -\zeta + 0.05y^2 \sin^2(y)$, $q_2 = -0.1\zeta + 0.1y^2 \cos^2(y)$, $f_{1,1} = f_{1,2} = 0$, $f_{2,1} = -\frac{Q}{P} \sin(x_1) - \frac{M}{P} x_2$, $f_{2,2} = -\frac{Q}{P} \sin(x_1) - \frac{M}{P} x_2 + 0.2 \sin(x_1) \cos(x_2)$, $f_{3,1} = -\frac{K_B}{PL} x_2 - \frac{R}{L} x_3$, $f_{3,2} = -\frac{K_B}{PL} x_2 - \frac{R}{L} x_3 + 0.1 \sin(x_1 x_2) \cos(x_3)$, $\Delta_{1,1} = 0.1 \sin(y\zeta) + 0.1e^{-t^2}$, $\Delta_{1,2} = 0.1 \cos(y\zeta) - 0.1e^{-t^2}$, $\Delta_{2,1} = 0.1 \sin(y\zeta^2) + 0.2 \sin(t^2)$, $\Delta_{2,2} = 0.1 \sin(y^2\zeta) + 0.2 \cos(t^4)$, $\Delta_{3,1} = \Delta_{3,2} = 0$, $h_1 = h_2 = 1$, $h_3 = \frac{1}{PL}$.

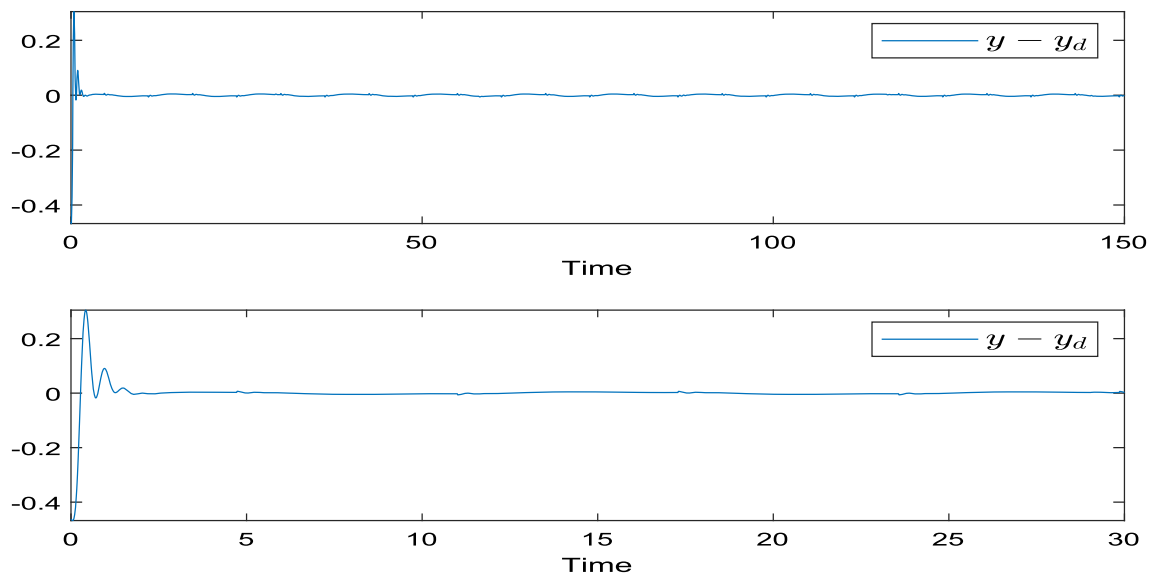


Fig. 19 Curve of tracking error $y - y_d$ for Example 2

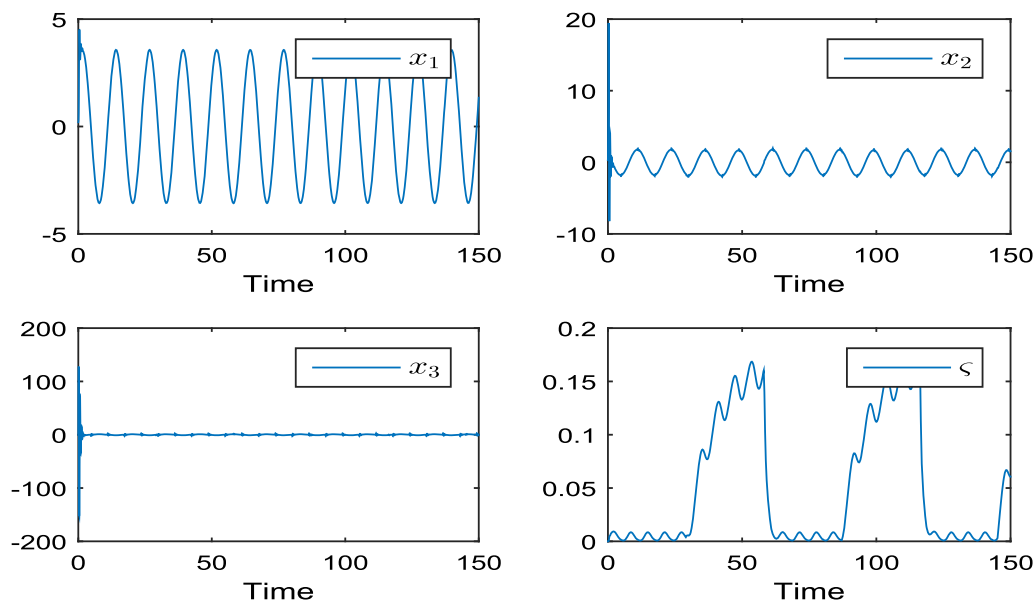


Fig. 20 Curves of x_1 , x_2 , x_3 and ζ for Example 2

In this example, $y_d = 0.5 \cos(0.5t) + \sin(0.5t)$. Select the initial conditions $x_1(0) = 0.2$, $x_2(0) = 0.3$, $x_3(0) = -0.2$, $\hat{\zeta}_1(0) = \hat{\zeta}_2(0) = \hat{\zeta}_3(0) = 0$, $\hat{\theta}(0) = 0$, $\hat{\beta}(0) = 0.03$. We choose $\mu_{1,1} = \mu_{1,2} = 3$, $\mu_{2,1} = \mu_{2,2} = 5$, $\mu_{3,1} = \mu_{3,2} = 2$, $\tau_a = 29.03 > \ln 13.8392/0.0905$. $l = 0.2$, $\nu = 0.01$, $j_1 = 2.5$, $h = 0.1$, $\iota = 0.001$, $a_1 = 2$, $a_2 = 1$, $a_3 = 3$, $s_1 = s_2 = s_3 = 2$, $c_1 = 4$, $c_2 = 9$, $c_3 = 120$. The simulation results are given in Figs. 18, 19, 20, 21, 22, 23,

24, and 25. The trajectories of y and y_d are depicted in Figs. 18, and 19 shows curve of the tracking error, we can see that the tracking error tends to be in a small neighborhood of the origin. Figure 20 shows curves of x_1 , x_2 , x_3 and ζ . Figure 21 shows curves of $\hat{\zeta}_1$, $\hat{\zeta}_2$, and $\hat{\zeta}_3$. Figure 22, 23 and 24 depict adaptive parameters $\hat{\theta}$, $\hat{\beta}$ and control input u , respectively. Figure 25 shows the switching signal.

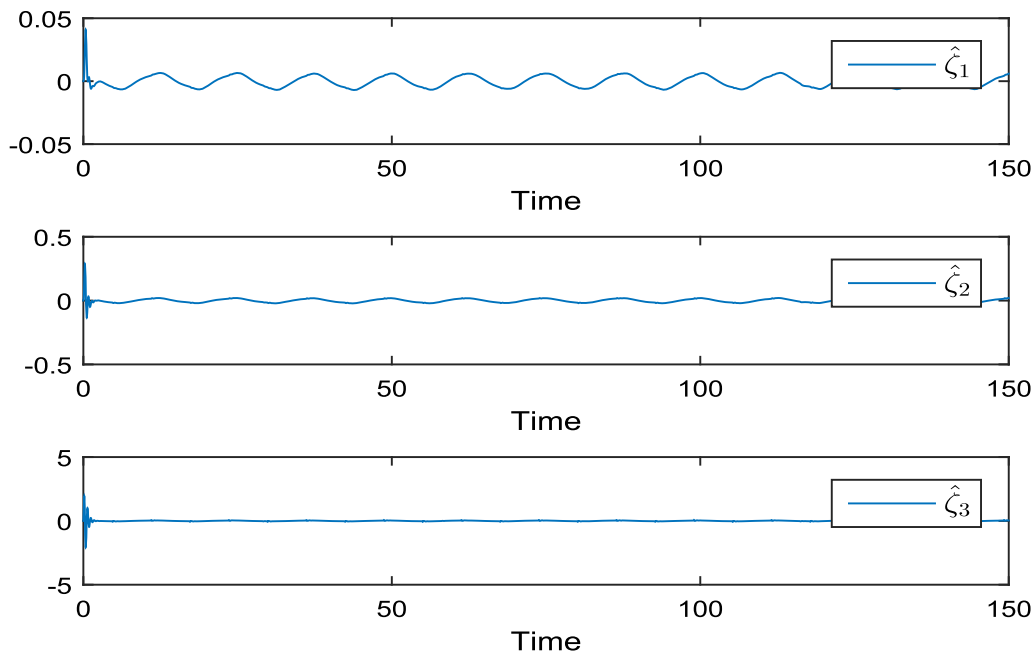


Fig. 21 Curves of $\hat{\zeta}_1$, $\hat{\zeta}_2$ and $\hat{\zeta}_3$ for Example 2

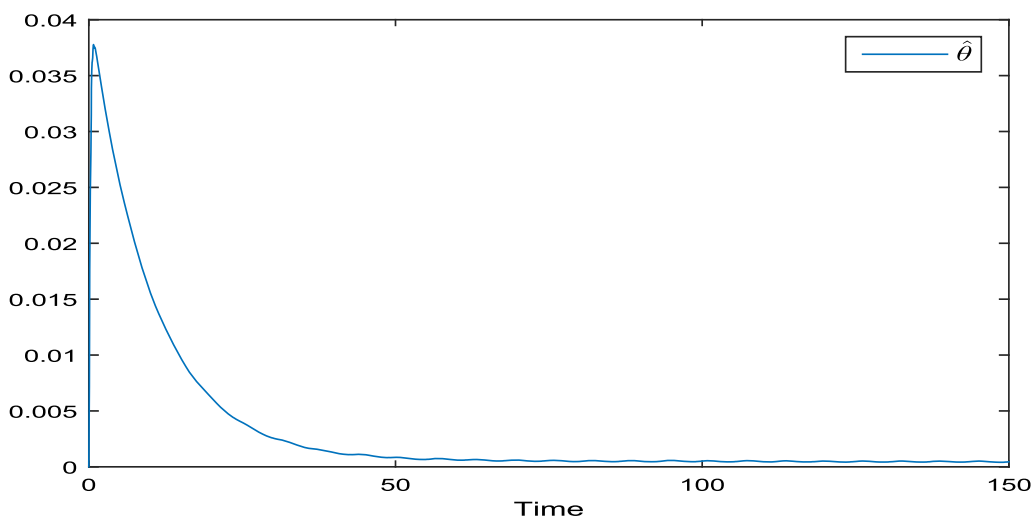


Fig. 22 Curve of $\hat{\theta}$ for Example 2

5 Conclusions

In this paper, the problem of adaptive fuzzy PI output feedback tracking control for a class of uncertain switched nonlinear systems with unmodeled dynamics, unknown control coefficients and dead-zone output has been

addressed. The proposed controller has a PI structure, which constitutes a more intuitive structure and has a stronger physical sense. The boundedness of all signals and tracking error of the closed-loop system has been analyzed using the Lyapunov stability theory. The validity of the scheme has been demonstrated through two examples.

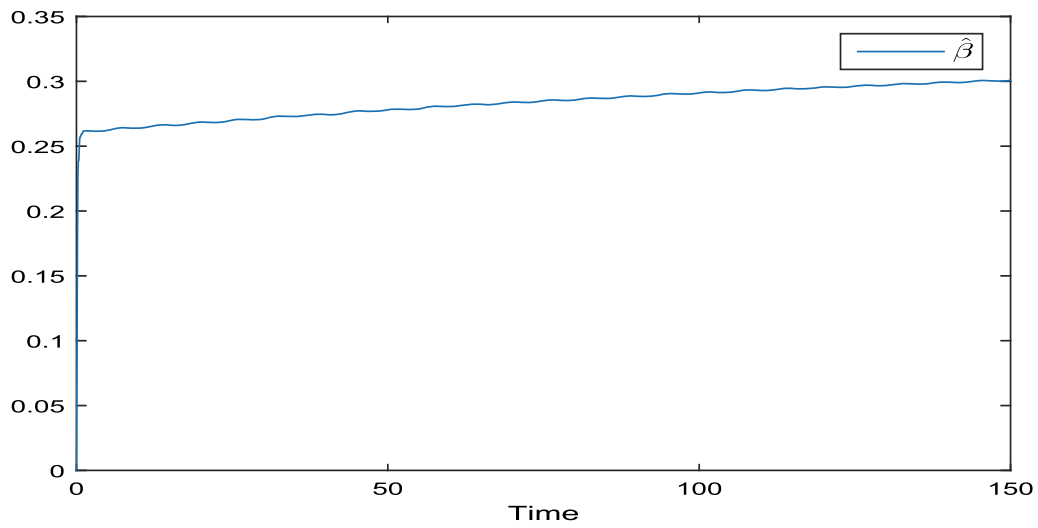


Fig. 23 Curve of $\hat{\beta}$ for Example 2

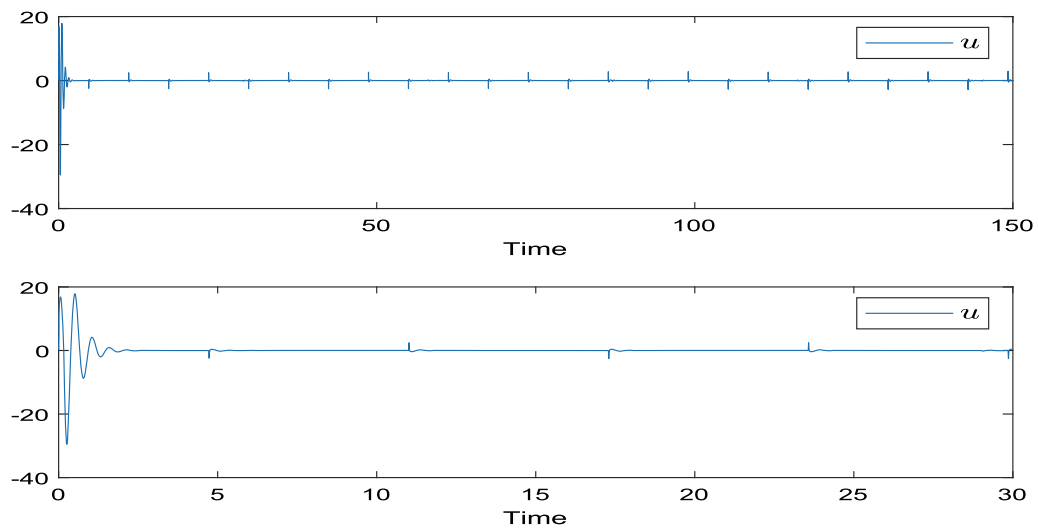


Fig. 24 Curve of control input u for Example 2

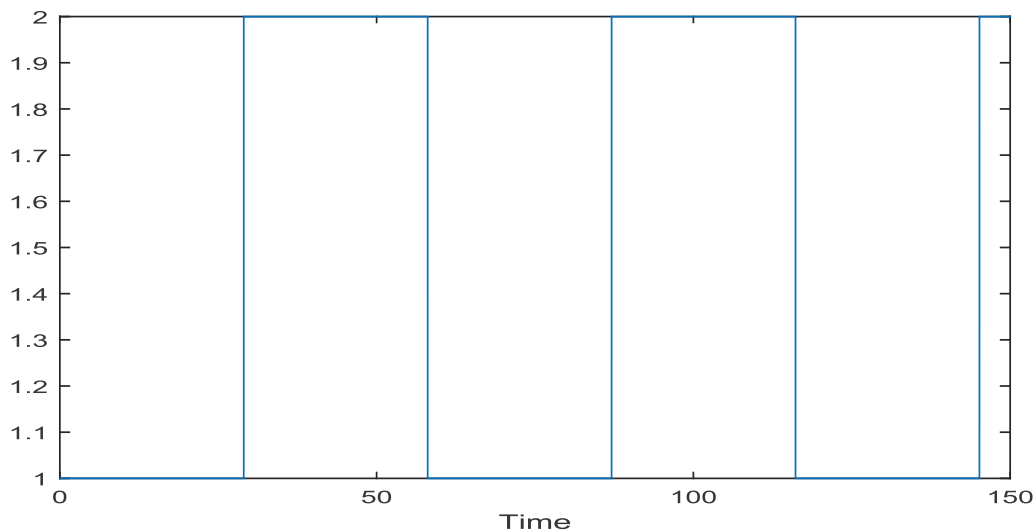


Fig. 25 Curve of the switching signal for Example 2

Acknowledgements This work is partially supported by the National Natural Science Foundation of China under Grant (61773236, 62173205, 61773235, 61703233, 61873331, 61803225), partially by the Natural Science Foundation Program of Shandong Province (ZR2020YQ48), partially by the Taishan Scholar Project of Shandong Province under Grant (TSQN20161033), partially by the Natural Science Foundation of Anhui Provincial (1908085MF219) and partially by Postdoctoral Science Foundation of China (2017M612236, 2019T120574).

References

- Zhao, Q.J., Chen, X.M., Li, J., Wu, J.: Finite-time adaptive fuzzy DSC for uncertain switched systems. *Int. J. Fuzzy Syst.* **22**, 2258–2270 (2020)
- Ma, L., Huo, X., Zhao, X.D., Zong, G.D.: Adaptive fuzzy tracking control for a class of uncertain switched nonlinear systems with multiple constraints: a small-gain approach. *Int. J. Fuzzy Syst.* **21**, 2609–2624 (2019)
- Li, Y.M., Tong, S.C., Liu, L., Feng, G.: Adaptive output-feedback control design with prescribed performance for switched nonlinear systems. *Automatica* **80**, 225–231 (2017)
- Hwang, C., Chen, Y.: Fuzzy fixed-time learning control with saturated input, nonlinear switching surface, and switching gain to achieve null tracking error. *IEEE Trans. Fuzzy Syst.* **28**(7), 1464–1476 (2020)
- Zhao, X., Wang, X., Ma, L., Zong, G.: Fuzzy approximation based asymptotic tracking control for a class of uncertain switched nonlinear systems. *IEEE Trans. Fuzzy Syst.* **28**(4), 632–644 (2020)
- Zhang, A., Deng, C.: Fuzzy adaptive fault-tolerant control for non-identifiable multi-agent systems under switching topology. *Int. J. Fuzzy Syst.* **22**, 2246–2257 (2020)
- Zong, G.D., Li, Y.K., Sun, H.B.: Composite anti-disturbance resilient control for Markovian jump nonlinear systems with general uncertain transition rate. *Sci. China Inf. Sci.* **62**, 22205 (2019)
- Long, L.J., Zhao, J.: H_∞ control of switched nonlinear systems in p -normal form using multiple Lyapunov functions. *IEEE Trans. Autom. Control* **57**(5), 1285–1291 (2012)
- Li, Y.M., Tong, S.C.: Adaptive fuzzy output-feedback stabilization control for a class of switched nonstrict-feedback nonlinear systems. *IEEE Trans. Cybern.* **47**(4), 1007–1016 (2017)
- Zhang, W., Wang, T.C., Tong, S.C.: Event-triggered control for networked switched fuzzy time-delay systems with saturated inputs. *Int. J. Fuzzy Syst.* **21**, 1455–1466 (2019)
- Zhai, D., Xi, C.J., An, L.W., Dong, J.X., Zhang, Q.L.: Prescribed performance switched adaptive dynamic surface control of switched nonlinear systems with average dwell time. *IEEE Trans. Syst. Man Cybern. Syst.* **47**(7), 1257–1269 (2017)
- Lai, G.Y., Liu, Z., Zhang, Y., Chen, C.L.P., Xie, S.L.: Adaptive backstepping-based tracking control of a class of uncertain switched nonlinear systems. *Automatica* **91**, 301–310 (2018)
- Zong, G.D., Ren, H.L., Karimi, H.R.: Event-triggered communication and annular finite-time H_∞ filtering for networked switched systems. *IEEE Trans. Cybern.* **51**(1), 309–317 (2021)
- Jiang, X.S., Tian, S.P., Zhang, W.H.: Weighted H_∞ performance analysis of nonlinear stochastic switched systems: a mode-dependent average dwell time method. *Int. J. Fuzzy Syst.* **22**, 1454–1467 (2020)
- Tang, X.N., Zhai, D., Fu, Z.M., Wang, H.M.: Output feedback adaptive fuzzy control for uncertain fractional-order nonlinear switched system with output quantization. *Int. J. Fuzzy Syst.* **22**, 943–955 (2020)
- Juan, M.T., Flavio, R., Ricardo, C., Paolo, F.: Switching control approach for stable navigation of mobile robots in unknown environments. *Robot. Comput. Integr. Manuf.* **27**(3), 558–568 (2011)
- Yang, C.G., Jiang, Y.M., Li, Z.J., He, W., Su, C.Y.: Neural control of bimanual robots with guaranteed global stability and motion precision. *IEEE Trans. Ind. Inf.* **13**(3), 1162–1171 (2017)
- Dixon, W.E., de Queiroz, M.S., Zhang, F., Dawson, D.M.: Tracking control of robot manipulators with bounded torque inputs. *Robotica* **17**(2), 121–129 (1999)
- Pellanda, P.C., Apkarian, P., Tuan, H.D.: Missile autopilot design via a multi-channel LFT/LPV control method. *Int. J. Robust Nonlinear Control* **12**(1), 1–20 (2002)
- Ligang, G., Qing, W., Chaoyang, D.: Switching disturbance rejection attitude control of near space vehicles with variable structure. *J. Syst. Eng. Electron.* **30**(1), 167–179 (2019)
- Wen, G., Yu, W., Hu, G., Cao, J., Yu, X.: Pinning synchronization of directed networks with switching topologies: A

- multiple lyapunov functions approach. *IEEE Trans. Neural Netw. Learn. Syst.* **26**(12), 3239–3250 (2015)
22. Donkers, M.C.F., Heemels, W.P.M.H., van de Wouw, N., Hetel, L.: Stability analysis of networked control systems using a switched linear systems approach. *IEEE Trans. Autom. Control* **56**(9), 2101–2115 (2011)
 23. Li, J., Wei, G., Ding, D., Li, Y.: Quantized control for networked switched systems with a more general switching rule. *IEEE Trans. Syst. Man Cybern. Syst.* **50**(5), 1909–1917 (2020)
 24. Ren, H., Zong, G., Li, T.: Event-triggered finite-time control for networked switched linear systems with asynchronous switching. *IEEE Trans. Syst. Man Cybern. Syst.* **48**(11), 1874–1884 (2018)
 25. Zhao, X.D., Zheng, X.L., Niu, B., Liu, L.: Adaptive tracking control for a class of uncertain switched nonlinear systems. *Automatica* **52**, 185–191 (2015)
 26. Li, Y., Tong, S.: Adaptive fuzzy output-feedback stabilization control for a class of switched nonstrict-feedback nonlinear systems. *IEEE Trans. Cybern.* **47**(4), 1007–1016 (2017)
 27. Zhai, D., Xi, C., An, L., Dong, J., Zhang, Q.: Prescribed performance switched adaptive dynamic surface control of switched nonlinear systems with average dwell time. *IEEE Trans. Syst. Man Cybern. Syst.* **47**(7), 1257–1269 (2017)
 28. Niu, B., Duan, P.Y., Li, J.Q., Li, X.D.: Adaptive neural tracking control scheme of switched stochastic nonlinear pure-feedback nonlower triangular systems. *IEEE Trans. Syst. Man Cybern. Syst.* **51**(2), 975–986 (2021)
 29. Jeong, D.M., Yoo, S.J.: Adaptive event-triggered tracking using nonlinear disturbance observer of arbitrarily switched uncertain nonlinear systems in pure-feedback form. *Appl. Math. Comput.* **407**, 126335 (2021)
 30. Rohrs, M. Athans., C.E., Valavani, L.S., Stein, G. : Robustness of adaptive control algorithms in the presence of unmodeled dynamics. *IEEE Trans. Autom. Control* **30**(9), 881–889 (1985)
 31. Tong, S., Li, Y.: Adaptive fuzzy output feedback control for switched nonlinear systems with unmodeled dynamics. *IEEE Trans. Cybern.* **47**(2), 295–305 (2017)
 32. Lyu, Z., Liu, Z., Xie, K., Chen, C.L.P., Zhang, Y.: Adaptive fuzzy output-feedback control for switched nonlinear systems with stable and unstable unmodeled dynamics. *IEEE Trans. Fuzzy Syst.* **28**(8), 1825–1839 (2020)
 33. Hua, C., Liu, G., Li, L., Guan, X.: Adaptive fuzzy prescribed performance control for nonlinear switched time-delay systems with unmodeled dynamics. *IEEE Trans. Fuzzy Syst.* **26**(4), 1934–1945 (2018)
 34. Hua, C., Liu, G., Li, Y., Guan, X.: Adaptive neural tracking control for interconnected switched systems with non-iss unmodeled dynamics. *IEEE Trans. Cybern.* **49**(5), 1669–1679 (2019)
 35. Li, H.Y., Sun, H.B., Hou, L.L.: Adaptive fuzzy PI output feedback bounded control for a class of switched nonlinear systems with input constraint. *Int. J. Syst. Sci.* **51**(16), 3503–3522 (2020)
 36. Ma, Z., Ma, H.: Improved adaptive fuzzy output-feedback dynamic surface control of nonlinear systems with unknown dead-zone output. *IEEE Trans. Fuzzy Syst.* **29**, 2122–2131 (2020)
 37. Shi, X., Lim, C., Shi, P., Xu, S.: Adaptive neural dynamic surface control for nonstrict-feedback systems with output dead zone. *IEEE Trans. Neural Netw. Learn. Syst.* **29**(11), 5200–5213 (2018)
 38. Ma, L., Huo, X., Zhao, X.D., Niu, B., Zong, G.D.: Adaptive neural control for switched nonlinear systems with unknown backlash-like hysteresis and output dead-zone. *Neurocomputing* **357**, 203–214 (2019)
 39. Davison, E.: Multivariable tuning regulators: the feedforward and robust control of a general servomechanism problem. *IEEE Trans. Autom. Control* **21**(1), 35–47 (1976)
 40. Gawthrop, P.: Self-tuning PID controllers: algorithms and implementation. *IEEE Trans. Autom. Control* **31**(3), 201–209 (1986)
 41. Khalil, H.K.: Universal integral controllers for minimum-phase nonlinear systems. *IEEE Trans. Autom. Control* **45**(3), 490–494 (2000)
 42. Agee, J.T., Kizir, S., Bingul, Z.: Intelligent proportional-integral (iPI) control of a single link flexible joint manipulator. *J. Vib. Control* **21**(11), 2273–2288 (2013)
 43. Agee, J.T., Bingul, Z., Kizir, S.: Tip trajectory control of a flexible-link manipulator using an intelligent proportional integral (iPI) controller. *Trans. Inst. Meas. Control.* **36**(5), 673–682 (2014)
 44. Song, Y.D., Guo, J.X., Huang, X.C.: Smooth neuroadaptive PI tracking control of nonlinear systems with unknown and nonsmooth actuation characteristics. *IEEE Trans. Neural Netw. Learn. Syst.* **28**(9), 2183–2195 (2017)
 45. Song, Q., Song, Y.D.: Generalized PI control design for a class of unknown nonaffine systems with sensor and actuator faults. *Syst. Control Lett.* **64**, 86–95 (2014)
 46. Song, Y.D., Shen, Z.Y., He, L., Huang, X.C.: Neuroadaptive control of strict feedback systems with full-state constraints and unknown actuation characteristics: an inexpensive solution. *IEEE Trans. Cybern.* **48**(11), 3126–3134 (2018)
 47. Sun, H.B., Zong, G.D., Ahn, C.K.: Quantized decentralized adaptive neural network PI tracking control for uncertain interconnected nonlinear systems with dynamic uncertainties. *IEEE Trans. Syst. Man Cybern. Syst.* **51**(5), 3111–3124 (2021)
 48. Jiang, Z.P.: A combined backstepping and small-gain approach to adaptive output feedback control. *Automatica* **35**(6), 1131–1139 (1999)
 49. Wang, L.X., Mendel, J.M.: Fuzzy basis functions, universal approximation, and orthogonal least-squares learning. *IEEE Trans. Neural Netw.* **3**(5), 807–814 (1992)
 50. Ge, S.S., Tee, K.P.: Approximation-based control of nonlinear MIMO time-delay systems. *Automatica* **43**(1), 31–43 (2007)
 51. Gu, H.B., Liu, K.X., Lv, J.H.: Adaptive PI control for synchronization of complex networks with stochastic coupling and nonlinear dynamics. *IEEE Trans. Circuits Syst. I Regul. Pap.* **67**(12), 5268–5280 (2020)
 52. Yao, B.: High performance adaptive robust control of nonlinear systems: a general framework and new schemes. In: *Proceedings of the 36th Conference on Decision and Control*, pp. 2489–2494 (1997)
 53. Hespanha, J.P., Morse, A.S.: Stability of switched systems with average dwell-time. In: *Proceedings of the 38th IEEE Conference on Decision and Control* (1999)
 54. Li, H.Y., Pan, Y.N., Shi, P., Shi, Y.: Switched fuzzy output feedback control and its application to a Mass-Spring-Damping system. *IEEE Trans. Fuzzy Syst.* **24**(6), 1259–1269 (2016)
 55. Xu, N., Wang, X.Y.: Adaptive fuzzy control design for a class of uncertain switched lower triangular systems. *Trans. Inst. Measur. Control* **40**(9), 2718–2723 (2018)
 56. Tong, S.C., He, X.L., Li, Y.M., Zhang, H.G.: Adaptive fuzzy back stepping Robust control for uncertain nonlinear systems based on small-gain approach. *Fuzzy Sets Syst.* **161**(6), 771–796 (2010)



Hongyao Li was born in Linyi, China, in 1996. He graduated from School of Mathematical Science, Liaocheng University with a bachelor's degree in 2018. Now he graduated from School of Engineering, Qufu Normal University with a master's degree in 2021. His current research direction is switched nonlinear systems.



Haibin Sun (M'17) was born in 1982. He is an associate professor in the School of Engineering at Qufu Normal University. He received his Ph.D degree in control theory and application from Southeast University in 2013. He was a Postdoctor with the School of Automation, Beihang University, Beijing, from 2013 to 2014. In 2017, he was a Visiting Scholar with the School of Engineering, RMIT University, Melbourne, Australia. In 2019,

he was a Visiting Scholar with the School of EEE, Nanyang

Technological University, Singapore. His research interests mainly lie in switched control, anti-disturbance control and its application.



Linlin Hou was born in 1982. She received her B.S., M.S., and Ph.D.degrees from Qufu Normal University, in 2006, 2009, and 2012,respectively. Since 2012, she has been with the School of Information Science and Engineering, Qufu Normal University, where she is currently a professor. Her main research interests include stability, control, and robustness analysis of switched system, Markovian jump system.